

Xylene Isomers Sorption on Zeolite Beta

Bakhta Abdelaziz

Dissertation submitted to the

School of Technology and Management of the Polytechnic Institute of Bragança

**To obtain a Master of Science Degree in Chemical Engineering in the scope of the double
degree program with the University of Saida**

Supervisor:

Doctor José António Correia Silva

Co- Supervisor:

Doctor MehdiAdjdir

Bragança

May 2020

Acknowledgments

I would like to show my sincere appreciation to those who have contributed to this dissertation and supported me in one way or the other during this amazing journey for without the generous support of them, this work would not have been possible.

First of all, I would like to express my pride to be supervised by widely known and highly experienced scientific researchers.

Professor Dr. José António Correia Silva and **Professor Dr. Mehdi Adjdir**, I am very thankful to have such a wonderful, professional and perfectionist persons as my thesis supervisors. I am deeply thankful for your continuous support and patience in this learning path, for your persistent help, and for the constant motivation to do more and better. You offered continuous advices and encouragement and I benefitted from your knowledge and scientific experience. I appreciate your effort and I want to thank you for your wise guidance, kindness and continuous availability.

Adriano Henrique my ultimate support. I am so grateful for everything that I have learned from you during my lab work time, your irreplaceable guidance and great help in laboratory procedures; you are a kind person; I would like to express my gratitude for all your support and encouragement. Thank you for always finding the time to guide me through all the difficult moments of research and while writing this thesis; thank you.

I also want to thank all researchers of the Mountain Research Centre (CIMO) for their support and generosity. Thank you all for always being so helpful and friendly, as well as for all your efforts and support during the realization of this work.

I am deeply grateful to all members of the jury who kindly honoured me by their presence to participate in the defence of this thesis.

My heartfelt gratitude goes to my wonderful and special friends, who assisted me in every way possible in achieving my dreams and successfully completing this research work. I will never forget all their support and effort. You're the best.

Keeping the best for last, I would like to dedicate To the spirit of my pure mother (**Hinda Nedjmi**) and thank my father **Ahmed Abdelaziz**, my sisters (**Chaima & Chahra**), and my fiancé (**Redouane**) whose help made this journey possible from the beginning they believe in me and supported my studies abroad both morally and financially. They have been my inspiration and my unfailing source of passion and energy. Thank you for your irreplaceable support, for all your love, patience and kindness, for always encouraging me to pursuit my education, for believing in me and for everything that you have done to make me the person I am now. Without you none of this would have been possible. I love you!!

INDEX

List of figures	iii
List of tables	v
List of abbreviations	vi
ABSTRACT	ix
I. INTRODUCTION.....	1
I.1 Motivation and outline.....	1
I.2 Objectives	3
II. STATE OF THE ART.....	4
II.1 Adsorption	4
II.1.1 Adsorption equilibrium isotherm models	5
Langmuir Equation.....	5
Dual-Site Langmuir (DSL).....	6
II.1.2 Isosteric Heat of Adsorption.....	6
II.1.3 Adsorbent	7
II.2 Xylene Isomers.....	9
II.2.1 The Importance of Separating Xylene and Ethylbenzene Isomers.....	10
II.2.2 the Para-, Meta- and Ortho-xylene	11
The Para-xylene.....	11
The Meta- and Ortho-xylene	12
II.2.3 Processes for the Separation of Xylene Isomers.....	12
II.3 Zeolites	15
II.3.1 Classification of Zeolites	17
II.3.2 Application	18
II.3.3 Zeolite beta.....	21

II.3.3.1 Synthesis.....	23
III. CHROMATOGRAPHY FRONTAL	25
III.1 Adsorption in Fixed Bed	25
III.1 Breakthrough curves measurements.....	28
IV. EXPERIMENTAL SECTION	29
IV.1 Characterization of Xylene and Ethylbenzene Isomers	29
IV.2 Characterization of the zeolite BETA under study	30
1. Scanning electron microscopy.....	30
2. Stereoscopy	32
3. X-ray diffraction.....	33
4. N ₂ Adsorption.....	34
5. The mercury porosimetry	34
IV.2.1 Activation and Preparation of the Zeolite BETA for Packing the Column	35
V. RESULTS AND DISCUSSION.....	40
V.1 Breakthrough Curves.....	40
V.2 Influence of Temperature on the Breakthrough Curves of Pure Components	43
V.3 Isotherms of Adsorption	44
V. 3.1 Adsorption Isotherms	44
V. 4 Comparison of Adsorption Isotherms	47
V. 5 Modeling of Experimental Data	49
V. 5.1 Modeling of Isotherm data	49
V. 6 Adsorption Enthalpies and Henry's Constant	55
VI. CONCLUSIONS	57
REFERENCES	58

List of figures

Figure 1 : Schematic diagram of UOP's PAREX process.	3
Figure 2 : Schematic representation of the adsorption process	4
Figure 3 : Pore size diameters classification according to IUPAC.	8
Figure 4 : Molecular structures of (a) o-xylene, (b) m-xylene and (c) p-xylene.....	9
Figure 5 : Crystals of laumontite and calcite in a cavity in an altered basalt near Kailua, northeast Oahu, Hawaii. This area is within the former conduit system of the 2.6 Ma Koolau volcano. It is likely that the pervasive rock alteration and zeolite formation is a result of hydrothermal activity when the volcano was active. The long dimension of the cavity is 8 cm.....	15
Figure 6 : Diagrams of elements of the frameworks of (a) the small-pore zeolite Rho, (b) the medium-pore zeolite ZSM-5, and (c) the large-pore zeolite Y. Tetrahedral (aluminum and silicon) cations are represented by small black spheres, and Oxygens are represented by larger spheres. Oxygens of selected rings that define access to the internal pore systems are highlighted in dark gray.....	16
Figure 7 : Zeolite beta framework and maximum free spheres fitting inside the channels.	21
Figure 8 : Framework structure of Beta zeolite (a) and SEM micrograph of Na-Beta-11 (b)..	23
Figure 9 : Example of a stoichiometric front for ideal fixed-bed adsorption.....	26
Figure 10 : Breakthrough curve for the sorption process in fixed beds C_o is the concentration of the inlet solution, C_b is the concentration of the breakthrough, t_b is the break point time and t_s is the saturation time.....	27
Figure 11 : Schematic representation of an experimental breakthrough curve and the adsorbed amount (q_0). (Bárcia, et al.2006).	28
Figure 12 : Representation of xylene isomers.	29
Figure 13 : Representation of ethylbenzene.	30
Figure 14 : (A) Zeolite beta pellets provided by Süd-Chemie AG (Si/Al=75). Scanning electron micrographs (SEM): (B) top view of the pellet (50×); (C) and (D) different view of transversal cut (15.000×).....	31
Figure 15 : Stereographic drawings and perspectives views of zeolite beta viewed along axis (a) [010], (b) [100] and (c) [001].	32

Figure 16 : XRD pattern of the commercial zeolite beta powder compared with the reference simulated pattern.....	33
Figure 18 : Schematic diagram of the adsorption equilibrium apparatus used to measure adsorption equilibrium data: (MFC) mass flow controller; (SP) syringe pump; (AC) adsorption column; (EC) expansion column; (EPC) electronic pressure control; (TCD) thermal conductivity detector; (V1) 3-way ball valve; (V2) flow metering valve, (BF) bubble flowmeter, and (①②③④) streams.	36
Figure 19 : Real view of the adsorption equilibrium apparatus: a) detailed view of the components system, and b) close-up inside the chromatograph oven.....	38
Figure 20 : Influence of temperature on breakthrough curves for p-xylene at the partial pressure of 0.100 bar	43
Figure 21 : Adsorption isotherms of p-xylene at three different temperatures.	44
Figure 22 : Adsorption isotherms of pure M-xylene components at three different temperatures.....	45
Figure 25 : Comparison of the pure component isotherms of the four aromatic compounds at 125°C.....	47
Figure 26 : Comparison of the pure component isotherms of the four aromatic compounds at 150°C.....	48
Figure 28 : Comparison of the fit of the DSL model to experimental data of the adsorption equilibrium of para-xylene.	51
Figure 29 : Comparison of the fit of the DSL model to experimental data of the adsorption equilibrium of Meta-xylene.	52
Figure 30 : Comparison of the fit of the DSL model to experimental data of the adsorption equilibrium of Ortho-xylene.	53
Figure 31 : Comparison of the fit of the DSL model to experimental data of the adsorption equilibrium of Ethylbenzene.....	54

List of tables

Table 1 : Composition and physical properties of xylene isomers and ethylbenzene and balancing.....	13
Table 2 : Physical Properties of C8 Aromatics.....	14
Table 3 : Zeolite structures with industrial application..	20
Table 4 : Conditions employed in the synthesis of zeolites.....	24
Table 5 : Kinetic diameters of the compounds present in the system.	30
Table 6 : Physical properties of zeolite beta crystals, mercury porosimetry data and N ₂ adsorption data of pellets.....	35
Table 7 : Operating conditions for fixed bed experiments performed with pure aromatic components (C ₈ H ₁₀) and respective adsorbed amounts.....	41,42
Table 8 : Parameters obtained for the isotherm models (Langmuir, DSL) regarding the adsorption of xylene isomers and ethylbenzene on Zeolite beta and the mean absolute deviations between the models and the experimental data.....	50
Table 9 : Adsorption enthalpies and Henry's constants for the isomers of xylene and ethylbenzene on Zeolite beta from the DSL model.....	55
Table 10 : Selectivities between the isomers of xylene and ethylbenzene, based on Henry's constants at 125, 150 and 175 °C, obtained by the DSL model.....	56

List of abbreviations

B	Langmuir constant or adsorption affinity constant, Pa ⁻¹
b₀	frequency factor of the affinity constant, Pa ⁻¹
BEA	Zeolite Beta
d_k	Kinetic diameter (nm)
DMT	dimethyl terephthalate
DSL	Dual-site Langmuir
EB	Ethylbenzene
EPC	Electronic Pressure Controller
FID	Flame ionization detector
IP	Injection port
IPI	Injection port ionizing
IUPAC	International Union of Pure and Applied Chemistry.
IZA	International zeolite Association
HPLC	high performance liquid chromatography
H	Henry's constant
IUPAC	International Union of Pure and Applied Chemistry
IZA	
MX	Meta-xylene
MFC	Mass flow controller
MIL	Materiaux Institut Lavoisier
MOF	Metal-organic framework
N	total number of measurements, dimensionless
OX	Ortho-xylene
P	Partial pressure (bar)
PBT	Polybutene of terephthalate
PET	Polyethylene terephthalate
PPT	Polypropylene terephthalate
PTA	Purified terephthalic acid
PX	Para-xylene
Q	amount adsorbed, g/100gads
q_s	saturation capacity of each type of sites, respectively, g/100gads

R	ideal gas constant, Pa m ³ mol ⁻¹ K
SBU	Secondary building unit
SEM	Scanning Electron Microscope
SMB	Simulated moving bed
SMBR	Simulated moving bed reactor
T	temperature, K
T	Time (min)
TCD	Thermal conductivity detector
UOP	Universal oil product
ZSM-5	Zeolite socony mobil-five

Symbols

	fractional loading (g/100gads)
ϵ_b	bed porosity

Gregorian Letters

ΔH	heat of adsorption, kJ/mol
ΔH_{st}	isosteric heat of sorption, kJ/mol
ΔH_0	Adsorption enthalpy at infinite dilution (KJ/mol)

Lower Indices

I	Component or counter
J	Component or counter
K	Component or counter
S	Saturation

Higher Indices

C	Relative to wide channels of Zeolite BETA
J	Relative to narrow Zeolite BETA channels

ABSTRACT

The separation of C₈ alkylaromatic mixed compounds is an important process in the chemical industry due to its direct connection with the manufacturing of PET (Polyethylene Terephthalate). The separation can be performed by distillation but the similarity of its boiling points increase significantly the cost. Alternatives are the crystallization and adsorption. In this work it is studied the ability of zeolite BETA to adsorb xylene isomers as a possible alternative adsorbent to the commonly used Faujasite zeolite or Y zeolite in the so called adsorptive process.

Zeolite BETA is an intergrowth of two or three polymorphs of crystalline microporous materials formed by tetrahedral corner-sharing TO₄ (T = Si or Al) in a unique porous structure with fine thermal and chemical stability. They have found wide spread applications in many industrial field such as catalysis, adsorption, separation, and ion exchange.

In this work it is studied the application of Zeolite BETA to separate xylene isomers in vapor phase by adsorption, through an experimental study to determine single component adsorption equilibrium isotherms of xylene isomers and ethylbenzene between the temperatures ranges from 125 to 175°C. The results obtained in this work are important for further studies in multicomponent systems regarding the ability of zeolite BETA to separate xylene isomers.

The adsorbed amount is higher at the lower temperature (125 °C) with values around 0.8 g/100g_{ads} and decrease with the increase temperature (175 °C). The adsorption hierarchy order is: EB > OX > PX > MX . The selectivity is very low but we could improve it with decrease the temperature.

KEYWORDS: Zeolite beta, xylene isomers separation, adsorption equilibrium, single component adsorption, isotherms, breakthrough.

RESUMO

A separação dos compostos alquilaromáticos C_8 é um processo importante na indústria química devido à sua ligação directa com o fabrico de PET (Polietileno Tereftalato). A separação pode ser feita por destilação - mas a semelhança dos seus pontos de ebulição aumenta significativamente o custo. As alternativas são a cristalização e a adsorção. Neste trabalho é estudada a capacidade do zeólito BETA de adsorver isómeros de xileno como possível adsorvente alternativo ao zeólito Faujasite ou zeólito Y comumente utilizado no chamado processo adsorvente.

O zeólito BETA é um intercrescimento de dois ou três polimorfos de materiais microporosos cristalinos formados por tetraédricos de partilha de cantos TO_4 (T = Si ou Al) numa estrutura porosa única com estabilidade térmica e química fina. Encontraram aplicações generalizadas em muitos campos industriais tais como a catálise, adsorção, separação e troca iónica.

Neste trabalho é estudada a aplicação do zeólito BETA para separar isómeros de xileno em fase de vapor por adsorção, através de um estudo experimental para determinar isómeros de isómeros de xileno e etilbenzeno em equilíbrio de adsorção de componente único entre as temperaturas de 125 a 175°C. Os resultados obtidos neste trabalho são importantes para estudos adicionais em sistemas multicomponentes relativamente à capacidade do zeólito BETA de separar os isómeros de xileno.

A carga adsorvida é maior à temperatura mais baixa (125 °C) com valores em torno de 0,8 g/100gads e diminui com a temperatura (175 °C): EB > OX > PX > MX. A selectividade é vista como muito baixa, mas pode mos dizer que quando a temperatura diminui.

PALAVRAS-CHAVE: Zeolite beta, separação de isómeros de xileno, equilíbrio de adsorção, adsorção de componente único, isotermas.

SOMMAIRE

La séparation des composés mixtes alkyl aromatiques en C8 est un processus important dans l'industrie chimique en raison de son lien direct avec la fabrication du PET (polyéthylène téréphtalate). La séparation peut être effectuée par distillation, mais la similitude des points d'ébullition augmente considérablement le coût. Les alternatives sont la cristallisation et l'adsorption. Dans ce travail, on étudie la capacité de la zéolite BETA à adsorber les isomères du xylène comme alternative possible à la zéolite Faujasite ou à la zéolite Y couramment utilisées dans le processus dit d'adsorption.

La zéolite BETA est une inter croissance de deux ou trois polymorphes de matériaux microporeux cristallins formés par le partage des coins tétraédriques TO_4 ($T = Si$ ou Al) dans une structure poreuse unique avec une fine stabilité thermique et chimique.¹⁻³ Ils ont trouvé des applications répandues dans de nombreux domaines industriels tels que la catalyse, l'adsorption, la séparation et l'échange d'ions.

Dans ce travail on étudie l'application de la zéolite BETA pour séparer les isomères du xylène en phase vapeur par adsorption, à travers une étude expérimentale pour déterminer les isothermes d'équilibre d'adsorption à un seul composant des isomères du xylène et de l'éthylbenzène entre les plages de températures de 125 à 175°C. Les résultats obtenus dans ce travail sont importants pour des études ultérieures dans des systèmes multi-composants concernant la capacité de la zéolite BETA à séparer les isomères du xylène.

La charge adsorbée est plus élevée à basse température (125 °C) avec des valeurs autour de 0.8 g/100gads et diminue avec la température (175 °C).L'ordre hiérarchique d'adsorption est : EB > OX > PX > MX. La sélectivité est très faible mais on peut dire qu'une amélioration apparaît avec la baisse de température.

MOTS CLÉS : zéolite bêta, séparation des isomères du xylène, équilibre d'adsorption, adsorption d'un seul composant, isothermes, advection.

I. INTRODUCTION

I.1 Motivation and outline

The most widely recognized benzene homologs with the general formula C_8H_{10} are mixed xylenes. The mixture of isomers consists primarily of three dimethylbenzene isomers (ortho-, meta-, and paraxylene) and ethylbenzene. The feedstocks used for the development of xylene give rise to a combination of the four isomers (Fabri, U. Graeser, T. Simo, 2002). Between the three isomers, px has the largest demand by far.

In fact, px is oxidized into terephthalic acid, which can be esterified into dimethyl terephthalate (a polyester precursor). Ox is oxidized into phthalic anhydride (plasticizer precursor) and mx into isophthalic acid (polyester precursor). Eb is dehydrogenated into styrene, converted to polystyrene and other polymers. These isomers boil together so carefully that it is not necessary to isolate them by traditional distillation (J.J. Jeanneret, A.R. Meyers, 1999).

Three primary processes: crystallization, adsorption, and a hybrid crystallization / adsorption process (M. Minceva, A.E. Rodrigues, 2007) are industrially conducted by p-x obtained from xylene blend. Approximately 60% of the p-x generated worldwide, however, is through adsorption technology.

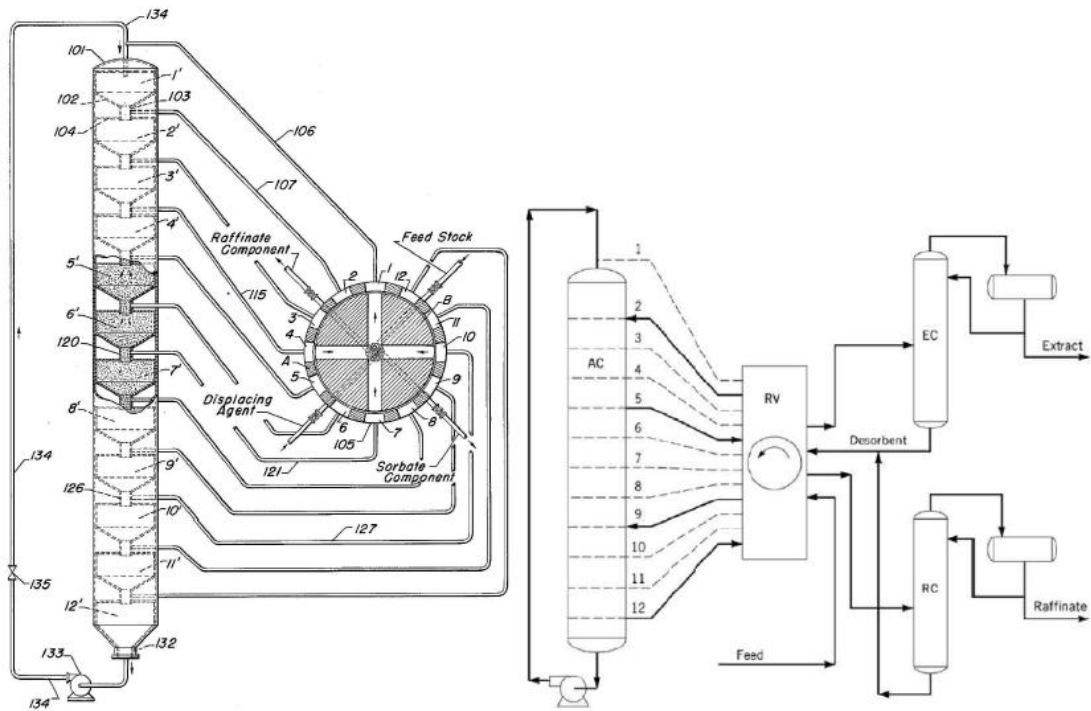
Zeolites are typical microporous crystalline materials with narrow pore size distribution ranging from 0.3 to 1.5 nm, having a widespread application in adsorption, separation, and catalysis with its unique properties, such as developed ordered porous structure, high specific surface area, and strong acidity, high hydrothermal and thermal stability (Baerlocher, C. et al., 2007; Degnan, T.F., 2000). As zeolite Beta has large window diameter and strong acidic sites, it has become a member of zeolitic materials of great substantial industrial importance, displaying unique catalytic reactivity in chemical reactions of hydrocarbons. Beta zeolite belongs to a complex intergrowth family, which consists of two (polymorph A and B) or more polymorphs (Newsam, et al., 1988). It is a high-silica zeolite with three-dimension channel system and consists of straight ring channels of a free aperture of 0.76×0.64 nm and zigzag ring channels of 0.55×0.55 nm which are similar to other large-pore molecular sieves such as FAU and EMT zeolites. Even Beta zeolite can be classified as a large pore zeolite with a 12-ring structure, it still suffers from strong steric and diffusion limitations from crystal sizes in

the micrometer range in a number of catalytic reactions with participation of bulky molecules (Brito, A. et al., 2007). Thus, it is important to develop mesoporous Beta zeolite which can improve the catalytic activities substantially in various organic reactions involving large molecules compared with microporous Beta zeolites.

Simulated Moving Bed (SMB) technology is used to perform adsorption separation, providing constant isolation using zeolites shared with cations such as Na^+ , K^+ , Ba^{2+} (Fabri, U. Graeser, T. Simo, 2002; D.M. Ruthven, M. Goddard, 1986). In order to provide tools for process understanding, operations and optimization, this process is being studied and simulated (M. Minceva, A.E. Rodrigues, 2007; P.S. Gomes, M. Minceva, A.E. Rodrigues, 2008). A Simulated Moving Bed Reactor (SMBR) implemented for p-xylene output, xylene isomerization integration and selective adsorption running in the liquid phase (Bergeot . G et al., 2010).

The separation of p-xylene by adsorption uses SMB (Simulated Moving Bed Chromatography) technology. A SMB is a continuous countercurrent process developed in the 1960s by UOP (Universal Oil Products). The SMB unit consists of a set of columns connected in series; the countercurrent flow of the solid and liquid phases is simulated by periodically changing the inlet (feed and desorbent) and outlet streams (extract and raffinate) in the direction of the fluid flow. Separation is accomplished by exploiting the differences in the affinity of the adsorbent for p-xylene relative to the other C_8 isomers.

In 1971, UOP commercialized the first Parex unit. **Fig 1** shows a diagram of a Parex unit.



(a) D.B. Broughton, C.G. Gerhold, (1961)

(b) Douglas M. Ruthven, (1984)

Figure 1 : Schematic diagram of UOP's PAREX process.

I.2 Objectives

The objectives of this work are:

- ✓ Study the ability of zeolite beta as an adsorbent for the separation of xylene isomers.
- ✓ Measure adsorption equilibrium isotherms by performing a set of single breakthrough experiments and determine selectivities.
- ✓ Modeling the adsorption equilibrium data.

II. STATE OF THE ART

II.1 Adsorption

In the 18th century, the ability of porous solids to reversibly adsorb large volumes of steam was recognized and the first experiments were carried out by Scheele and Fontana (Mc Brain, 1932), but at the level of separation and purification, the functional use of this property for large-scale industrial projects is comparatively recent (nicolao,2008). The first concrete steps were made in the 1950s with the use of adsorption as a way of splitting mixtures into two or three sources, each enriched with a value-added compound they would like to retrieve.

The first examples in this area were provided in 50s with the Arosorb method for the recovery of aromatic hydrocarbons (Davis et al., 1952) and with a variety of processes. At the beginning of the 1960s, adsorption was used to distinguish linear paraffins from branched and cyclic isomers. There was a substantial growth in the range and size of these processes in the 1970s. **Fig 2** shows the pattern of the adsorption process.

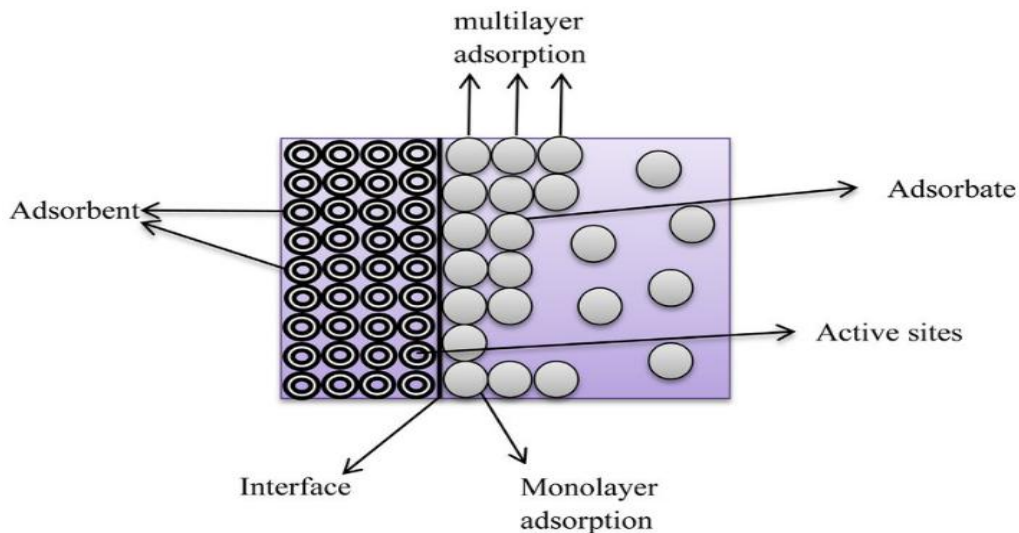


Figure 2 : Schematic representation of the adsorption process (Soliman, n.k and Moustafa, Ahmed, 2020).

II.1.1 Adsorption equilibrium isotherm models

Irrespective to the number of components present in a given mixture, the adsorption equilibrium of pure components is a crucial ingredient in the understanding of how these components contact with the solid adsorber. This knowledge can be used in the kinetic analysis of pure component adsorption, in the adsorption balance of multicomponent systems, and later in the adsorption kinetics of multicomponent systems (Duong, 1998).

Langmuir Equation

Langmuir (1918) was one of the first to develop a coherent theory for the description of adsorption equilibrium.

The assumptions of Langmuir's theory are the following:

1. The surface is homogeneous, the energy being constant in all sites.
2. The adsorption on the surface is located, the adsorbed atoms or molecules are adsorbed in localized and defined sites.
3. Each site can only accommodate a single molecule or atom, which should not interfere with the neighboring molecules or atoms.
4. Langmuir's theory is based on a kinetic principle.

The rate of adsorption correlates to surface desorption values. **(Eq 1)** is the Langmuir adsorption equilibrium equation. The equation presented is written in terms of quantity adsorbed (C. Malara, G. Pierini, A. Viola, 1992).

$$q = q_s \frac{bP}{1+bP} \quad (1)$$

Where

$$b = b_0 \exp\left(\frac{\Delta H_0}{RT}\right) \quad (2)$$

The letter q symbolizes the quantity of adsorbed (g/100 g ads), q_s symbolizes the overall quantity of adsorbed corresponding to the monolayer saturation, b represents the

constant affinity and is temperature-dependent and P represents the adsorbate partial pressure.

Another way to present the Langmuir equation is in terms of the fractional loading (θ).

$$\theta = \frac{bP}{1+bP} \quad (3)$$

The Langmuir isotherm is not always valid to describe the adsorption equilibrium, mainly on the assumption that all active surface sites have the same adsorption heat. If the surface is saturated, adsorption heat typically decreases, meaning that the surface is not homogeneous and more assets are filled as a matter of priority by adsorption sites (Choi, J.et al., 2006).

The parameters of the Langmuir equation can be obtained from **(Eq 1)** by transformation into a linear relation,

$$\frac{1}{q} = \frac{1}{q_s b P} + \frac{1}{q_s} \quad (4)$$

Dual-Site Langmuir (DSL)

Due to either the heterogeneity of active sites or the interaction of adsorbed molecules, deviations may occur to the Langmuir theory.

One of the variants due to energy heterogeneity of the adsorbent surface is the so-called Dual-Site Langmuir (DSL) model, **(Eq 5)**, which identifies two types of active sites in the solid, with each active site adopting a "Langmuirian" action (Yan, Y., Davis, M., and Gavalas, G. 1995).

$$q = q_s^C \frac{b^C P}{1+b^C P} + q_s^J \frac{b^J P}{1+b^J P} \quad (5)$$

II.1.2 Isotheric Heat of Adsorption

The isotheric heat of adsorption, which is the ratio between the infinitesimal difference in the adsorbate enthalpy and the infinitesimal variation in the adsorbed quantity, is one important property to be evaluated for adsorption studies.

Isosteric heat may or may not differ with the amount of adsorption and is measured using the van't Hoff thermodynamics equation below:

$$\frac{\Delta H_{st}}{RT^2} = -\left(\frac{\partial \ln P}{\partial T}\right)_q \quad (6)$$

II.1.3 Adsorbent

One of the steps in the development of adsorption processes is the choice of a suitable adsorbent. To achieve a high degree of adsorption, an adsorbent must have a high specific area, since the higher the surface area, the better will be the adsorption. The larger is this surface area; the better is the capacity of the particle to adsorb the molecules.

Many solids have the ability to adsorb gas and liquid species, but few possess the selectivity to make them commercial adsorbents. For an adsorptive process, it is not enough for an adsorbent to have a high surface area. An adsorbent used in the industrial process must have high adsorption capacity, high selectivity, regenerability, high mechanical strength, good thermal stability and good stability under operational conditions (temperatures and pressures...).

Commercial adsorbents can be purchased in the form of granules, spheres, cylindrical pellets and powders of various sizes (Bárcia, et al., 2003). This division is somewhat arbitrary when taking into consideration the pore size of the pore that is relative to the size of the molecule to be adsorbed. By the definition of IUPAC (International Union of Pure and Applied Chemistry), a micropore has a diameter less than 2 nm, a mesopore has an average diameter from 2 to 50 nm and a macroporous has larger diameter which is more than 50 nm, as can be seen in **Fig 3**.

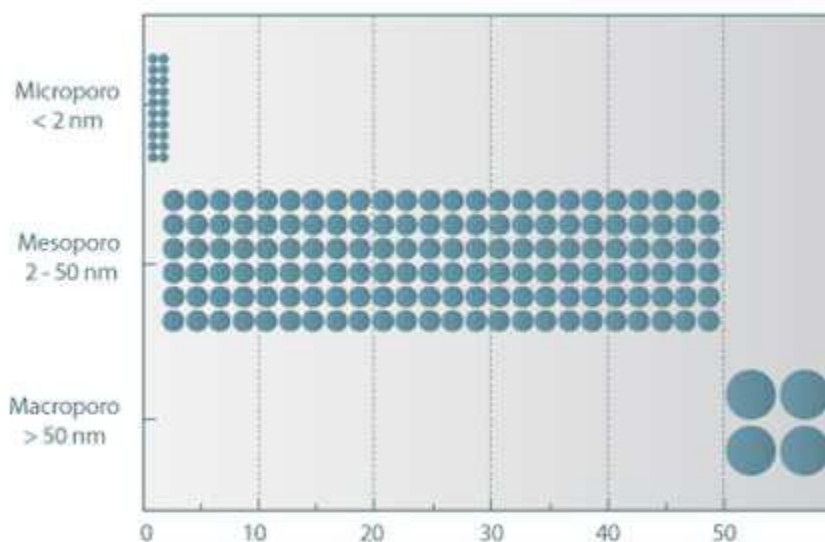


Figure 3 : Pore size diameters classification according to IUPAC.

The development of a new adsorbent in the industry usually goes through several steps: design and preparation of the materials, selective gas adsorption studies, evaluation of the materials, design and optimization.

II.2 Xylene Isomers

Xylene isomers are aromatic compounds derived from petroleum oil. The molecular structure of these isomers consists of one benzene ring and two methyl groups bound to the ring in three distinct positions. The word xylene is widely used to designate the industrial combination of the three isomers, ortho-xylene, meta-xylene and para-xylene; or 1,2-dimethylbenzene, 1,3-dimethylbenzene and 1,4-dimethylbenzene, respectively (Yang Yuxi et al., 2017). Because these compounds are isomers and have identical physicochemical properties, the process of producing pure isomers is complex. Its related industrial applications, especially in the plastics industry, have led to the development of a number of studies focusing on the use of new materials. These studies have the goal of refining current processes that aim to acquire pure isomers, with a focus on improving the separation performance of xylene isomers.

Xylene isomers are derived from the catalytic phase of naphtha reformation resulting from the main distillation of petroleum. In this process, isomers are isolated from other hydrocarbons by a catalytic wheel containing platinum halogen. The development of pure xylene by the petrochemical industry begins with the isolation of a fraction composed of eight carbon atom hydrocarbons, the C₈ fraction that feeds the xylene column.

The effluent from this xylene column will then be fed to the PAREX unit to obtain p-xylene (extract). The refined oil is pumped into the ISOMAR unit, where the isomers are converted into p-xylene. After this point, the unused materials returned to the xylene column (Meyers, 2003).

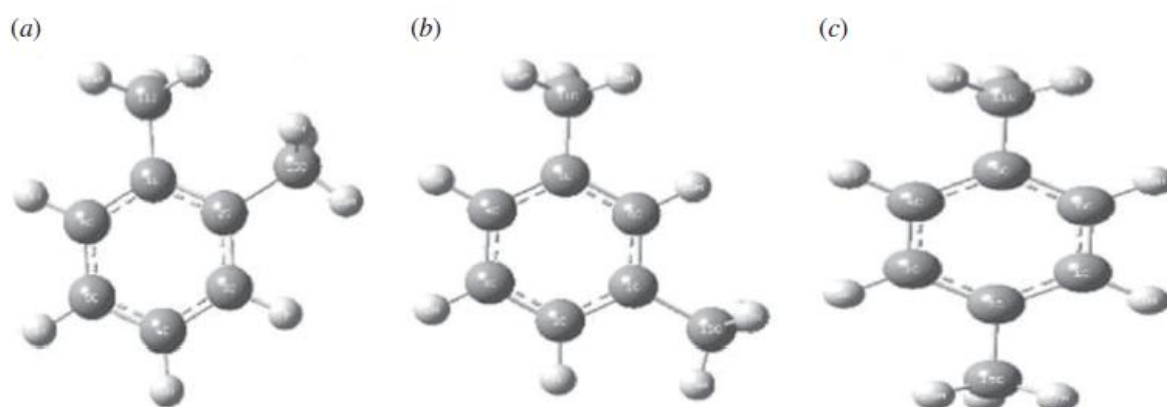


Figure 4 : Molecular structures of (a) o-xylene, (b) m-xylene and (c) p-xylene (Muhammad Farooq Saleem Khan and al., 2018).

Xylene isomers are used in the manufacture of different derivatives on a commercial level as solvents or intermediates. The principal isomer is p-xylene, which is used to produce polyesters after oxidation to terephthalic acid. Polyester films and fibers are being used to stretch quickly (Deckman et al., 2007).

There is a mixture of xylene and ethylbenzene isomers in the sources used for xylene processing (catalytic reformat, gasoline pyrolysis and toluene dispersion). The separation of these isomers is a classic issue in the petrochemical sector and the isolation by distillation is inefficient and economically impossible because of their near boiling points (Alirio E. Rodrigues, Mirjana Minceva, 2005).

Selective adsorption has been proposed to satisfy current an alternative to traditional separation methods. The petrochemical industry has a significant interest in xylene isomers being separated and purified by means of selective adsorption on zeolites.

II.2.1 the Importance of Separating Xylene and Ethylbenzene Isomers

Xylenes are used on a large scale as industrial solvents or intermediates for various derivatives. The most important isomer is p-xylene, which after being oxidized to terephthalic acid is used in the production of polyesters (Minceva, et al., 2003). This isomer has great industrial importance, since it is used as a raw material in the manufacture of polyethylene terephthalate (PET), in the production of polyester fibers plastics, films, and plastic beverage bottles. Therefore, the separation of PX from C8 aromatics has become a large-scale process in industry (Guo, et al., 2000).

The interest of the separation of ox from its isomers at the industrial level is due to its use in the production of phthalic acid, which can be obtained by catalytic oxidation with oxygen. Phthalic acid in its anhydrous form is used widely in industry for the production of dyes, insecticides, plasticizers and pharmaceuticals; it is also used in analytical chemistry (Wang Jyue-Sheng 1965).

The major industrial use of m-xylene is the manufacture of phthalic acid, which is used as a copolymer to the PET, providing a more suitable PET material for the manufacture of soft drink bottles.

Ethylbenzene is very important to the petrochemical industry as an intermediate in the production of styrene. Although it is often present in small quantities in crude oil, ethylbenzene is produced in large quantities by combining benzene with ethylene in a chemical reaction. (Daniela, 2009).

II.2.2 the Para-, Meta- and Ortho-xylene

The Para-xylene

Para-xylene or more generally, p-xylene (PX) is an aromatic hydrocarbon based on a benzene ring containing two methyl replacements. P stands for and specifies the role of the methyl group which in the case of PX, is at positions 1 and 4 respectively. The IUPAC name is 1,4-dimethylbenzene. Of the three isomers, PX has the highest market, largely due to the polyester industry. PX is mostly used for the processing of distilled terephthalic acid (PTA) and terephthalate esters, such as dimethyl terephthalate (DMT), which is used in the construction of various polymers such as Polyethylene terephthalate (PET), polypropylene terephthalate (PPT) or polybutylene terephthalate (PBT). Various grades of PET are used for a wide variety of common consumer products, such as film, synthetic fiber and plastic bottles for drinks. PPT and PBT can be used to render identical goods with different properties (Deckman et al., 2007).

The PX dime, di-p-xylene, when polymerized forms Parylene. In electronics, the low-pressure chemical vapor deposition of Parylene produces a thin film of adaptive insulation. Parylene coating has a high electrical resistance and is resistant to moisture infiltration. One of the most recent uses of Parylene is in pharmaceutical applications to have an inert buffer against moisture, toxins, bio-fluids and biogas (Yuxi Yang et al., 2017).

It also has a high degree of bio-compatibility required for implants and other long-term applications. It is used as a dielectric in certain high-performance capacitors for precise calculation. It is also used for the storage of document records.

The Meta- and Ortho-xylene

m-xylene (mX) is an aromatic hydrocarbon based on a benzene ring comprising two methyl equivalents in positions 1 and 3 of the aromatic ring. The IUPAC name is 1,3-dimethylbenzene. Economic interest in this isomer is due to its use in the manufacture of isophthalic acid or benzene-1, 3-dicarboxylic acid, and an aromatic dicarboxylic acid with the chemical formula $C_6H_4(COOH)_2$. It is an isomer of phthalic acid and terephthalic acid and can be obtained by oxidation of MX with chromium. Isophthalic acid is used as a copolymer to change the properties of polyethylene terephthalate (PET) and to make PET more suitable for the manufacturing of soft drink bottles (Deckman et al. 2007)

The distinction with the other isomer, o-xylene (OX), is that the two methyl replacements are in the 1 and 2 aromatic rings. Its IUPAC designation is 1,2-dimethylbenzene. OX is commonly used in the manufacture of phthalic acid, which can be produced by catalytic oxidation of OX with oxygen. Phthalic anhydride in its anhydrous nature is commonly used in the agricultural processing of dyes, insecticides, plasticizers and pharmaceuticals, often used in analytical chemistry.

II.2.3 Processes for the Separation of Xylene Isomers

The isolation of xylene isomers is a classic issue in the petrochemical industry since its boiling points are very close. The first separation methods were focused on the isolation and crystallization of solvents (Minceva et al., 2003).

The raw materials used in the manufacture of xylene (catalytic reformed, gasoline pyrolysis, toluene dismutation) include a combination of xylene and ethylbenzene (EB) isomers. The standard balance compositions of these compounds in the separator power supply are presented in Table 1 (Alirio E. Rodrigues, Mirjana Minceva, 2005).

Fractional distillation is a common process used in many industrial plants to isolate chemical compounds using physical properties as the boiling point. Can be used for the separation of OX and probably EB, but it cannot be used for the separation of PX. However it is also difficult to use this technology as traditional fractional distillation to isolate EB and the different xylene isomers effectively and economically.

This is because the boiling points of the four aromatics are within a very small range of 8 °C, from 136 °C to 144 °C (see **Table 1**).

Table 1: Composition and physical properties of xylene isomers and ethylbenzene and balancing. (Krishna, R. 2015).

C8 compounds	mass composition(%)	boiling point (°C)	melting point (°C)
Ethylbenzene	14.0	136	-95
Meta-xylene	49.7	139	-48
Ortho-xylene	12.7	144	-25
Para-xylene	23.6	138	13

The PX and MX boiling points are only 1 °C apart. As a result, it would be necessary to large equipment, significant energy consumption and/or substantial recycling in order to obtain separations of effective and satisfactory xylenes. Nevertheless, several methods and processes, other than the simple fractional distillation have been developed and tested to separate these C8 aromatic compounds and some are successfully practiced on an industrial scale. Examples include fractional crystallization, adsorption and combinations of these. Fractional crystallization in a crystallizer that takes advantage of the significant differences between the melting points of C₈ aromatic compounds.

The Separation of xylene isomers has been thought of as one of seven world-changing separations. highly challenging as a result of the similar physicochemical properties of these isomers (**Table 2**).

Table 2 : Physical Properties of C8 Aromatics (Yuxi Yang and al., 2017).

Parameters	PX	MX	OX	EB
Kinetic diameter (Å)	6.7	7.1	7.4	6.7
boiling point (K)	411.5	412.3	417.6	409.3
freezing point (K)	286.4	222.5	248.0	178.2
dipole moment (D)	0	0.36	0.62	0.59
polarizability (cm³)	13.7	14.2	14.9	14.2
density at 298 K (g cm⁻³)	0.858	0.861	0.876	0.867

II.3 Zeolites

Zeolites are aluminosilicate minerals that occur as low-temperature (generally less than 200 °C) alteration products of volcanic and feldspathic rocks. They are well known in cavities of basalt, having crystallized as a result of diagenetic or hydrothermal alteration (**Fig 5**). Some zeolites completely replace rhyolitic tuff in saline alkaline lacustrine environments or through groundwater percolation. Thick sequences of sediment from arc-source terranes contain several different kinds of zeolite, which formed through diagenetic alteration and very low-grade metamorphism. These occurrences of zeolites have economic significance, because they either produce useful rock or affect the porosity of reservoir rocks.



Figure 5 : Crystals of laumontite and calcite in a cavity in an altered basalt near Kailua, northeast Oahu, Hawaii. This area is within the former conduit system of the 2.6 Ma Koolau volcano. It is likely that the pervasive rock alteration and zeolite formation is a result of hydrothermal activity when the volcano was active. The long dimension of the cavity is 8 cm. (W.S. Wise, 2005).

Zeolites are microporous aluminosilicates consisting of vertex-sharing aluminate and silicate tetrahedral . Each aluminum atom in the framework introduces a negative charge, which must be balanced by a charge-balancing cation or proton, which can act as a Lewis or Bronsted acid, respectively. The acid forms of zeolites have found wider use as acid catalysts than any other materials. Their

outstanding utility derives from their relatively high acid strength, their high hydrothermal stability, their ability to impart shape selectivity into product distributions, and the reproducibility with which they can be synthesized and modified. Each of these advantages stems directly from their crystalline structure.

Nearly 100 zeolite structure types are known, but only a handful is used commercially, due to economic and safety issues associated with syntheses of the more novel types. Some zeolites that have found application as solid acids are shown in **Fig 5**, grouped into small, medium, and large pore types. Access to the internal surfaces of small pore zeolites is controlled by openings bounded by rings containing eight tetrahedral cations and eight oxygens (eight-membered rings or 8MRs). Medium-pore zeolites, such as ZSM-5, possess pore systems bounded by 10MRs, and large-pore zeolites, such as zeolite Y, mordenite, and zeolite beta have pore systems bounded by 12MRs. Typical pore openings of 8MRs are 4 Å, of 10MRs 5–5.5 Å, and of 12MRs 7.5 Å.

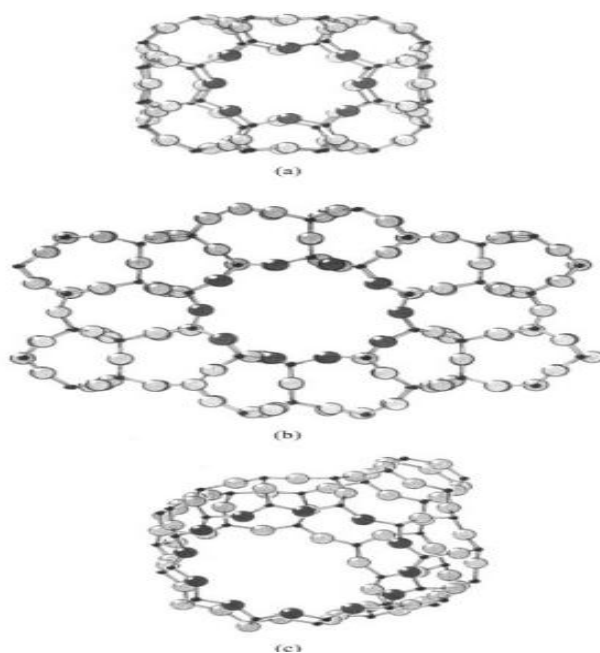


Figure 6 : Diagrams of elements of the frameworks of (a) the small-pore zeolite Rho, (b) the medium-pore zeolite ZSM-5, and (c) the large-pore zeolite Y. Tetrahedral (aluminum and silicon) cations are represented by small black spheres, and Oxygens are represented by larger spheres. Oxygens of selected rings that define access to the internal pore systems are highlighted in dark gray (A. Dyer, 2001).

II.3.1 Classification of Zeolites

More than 50 different species of this mineral group have been identified and still more to be identified. Zeolites have been classified on the basis of their morphological characteristics, crystal structure, chemical composition, effective pore diameter, natural occurrence, etc. In the year 1997, the subcommittee on zeolites of the International Mineralogical Association Commission on New Minerals and Mineral Names has recommended nomenclature for zeolite minerals. The report suggested that zeolite species are not to be distinguished solely on the ratio of Si to Al, except for heulandite (Si:Al < 4.0) and clinoptilolite (Si:Al \geq 4.0). Dehydration, partial hydration and over-hydration are not sufficient grounds for the recognition of separate species of zeolites (Coombs et al., 1997).

The Si/Al ratio is an important characteristic of zeolites. The charge imbalance due to the presence of aluminum in the zeolite framework determines the ion-exchange characters of zeolites and is expected to induce potential acidic sites. The Si/Al ratio is inversely proportional to the cation content, however directly proportional to the thermal stability. The surface selectivity changes from hydrophilic to hydrophobic when the ratio increases. Silica molecular sieves (silicalite-1) have a neutral framework; are hydrophobic in nature, and have no ion-exchange or catalytic properties.

Zeolites are classified on the basis of silica:alumina ratio as follows:

1. Zeolites with low Si:Al ratio (1.0 to 1.5)
2. Zeolites with intermediate Si:Al ratio (2 to 5)
3. Zeolites with high Si:Al ratio (10 to several thousands).

As the Si to Al ratio continues to increase, the catalytic activity often tends to pass through a maximum because of two opposing effects: increasing effectiveness of each acid center on the one hand, and decreasing number of acid centers on the other. The aluminous zeolites are excellent desiccants whereas the most siliceous zeolites tend to be organophilic non polar sorbents. Flanigen (1980) considered that “low silica” zeolites or aluminum-rich zeolites contain the maximum number of cation-exchange sites balancing the framework aluminum, and thus the highest cation contents; “intermediate silica” zeolites exhibit a common characteristic in terms of improved stability over the “low silica” zeolites and “high silica” zeolites representing heterogeneous hydrophilic surfaces within a porous crystal. The surface of the high

silica zeolites approaches a more homogeneous characteristic with an organophilic–hydrophobic selectivity and exchange capacities Flanigen (2001) has classified zeolites based on pore diameter, namely, small-pore zeolites, medium-pore zeolites, large-pore zeolites, and extra-large-pore zeolites:

- a. Small-pore zeolites (8-rings) with free pore diameter of 0.3–0.45 nm.
- b. Medium-pore zeolites (10-rings) with free pore diameter of 0.45–0.6 nm.
- c. Large-pore zeolites (12-rings) with free pore diameter of 0.6–0.8 nm
- d. Extra-large-pore zeolites (14-rings) with free pore diameter of 0.8–1.0 nm.

II.3.2 Application

Natural zeolite is a new and very good natural filter medium available for the filtration of water. It offers superior performance to sand and carbon filters, giving purer water and higher throughput rates with less maintenance required. It has many advantages over sand and can be used to directly replace sand in a normal sand filter.

There are three main uses of zeolites in industry: catalysis, gas separation and ion exchange. (Christopher J. Rhodes, 2010).

a. Catalysis: Zeolites are extremely useful as catalysts for several important reactions involving organic molecules. The most important are cracking, isomerization and hydrocarbon synthesis. Zeolites can promote a diverse range of catalytic reactions including acid-base and metal induced reactions. Zeolites can also be acid catalysts and can be used as supports for active metals or reagents. Zeolites can be shape-selective catalysts either by transition state selectivity or by exclusion of competing reactants on the basis of molecular diameter. They have also been used as oxidation catalysts. The reactions can take place within the pores of the zeolite, which allows a greater degree of product control. The main industrial application areas are: petroleum refining, synfuels production, and petrochemical production. Synthetic zeolites are the most important catalysts in petrochemical refineries.

b. Adsorption: Zeolites are used to adsorb a variety of materials. This includes applications in drying, purification, and separation. They can remove water to very low partial pressures and are very effective desiccants, with a capacity of up to more than 25% of their weight in water. They can remove volatile organic chemicals from air

streams, separate isomers and mixtures of gases. A widely used property of zeolites is that of gas separation. The porous structure of zeolites can be used to "sieve" molecules having certain dimensions and allow them to enter the pores. This property can be fine tuned by varying the structure by changing the size and number of cations around the pores. Other applications that can take place within the pore include polymerization of semi conducting materials and conducting polymers to produce materials having unusual physical and electrical attributes.

c. Ion exchange: Hydrated cations within the zeolite pores are bound loosely to the zeolite framework, and can readily exchange with other cations when in aqueous media. Applications of this can be seen in water softening devices, and the use of zeolites in detergents and soaps. The largest volume use for zeolites is in detergent formulations where they have replaced phosphates as water-softening agents. They do this by exchanging the sodium in the zeolite for the calcium and magnesium present in the water. It is even possible to remove radioactive ions from contaminated water.

Table 3 : Zeolite structures with industrial application. (Tanabe and Höelderich, 1999; Guisnet, 2002 and Vermeiren and Gilson, 2009).

IZA ^a code	Name	Channel dimensions (Å) ^b	Applications
AEL	AIPO4-11	4.0 x 6.5*	Cat
*BEA	Beta	6.6 x 6.7** ↔ 5.6 x 5.6*	Cat
CHA	Chabazite	↔ 3.8 x 3.8***	Ads
EDI	Edingtonite	2.8 x 3.8** ↔ 2.0 x 3.1*	Ads
ERI	Erionite	↔ 3.6 x 5.1***	Cat
EUO	EU-1	4.1 x 5.4*	Cat
FAU	Faujasite	7.4 x 7.4***	Cat / Ads
FER	Ferrierite	4.2 x 5.4* ↔ 3.5 x 4.8*	Cat
GIS	Gismondine	{3.1 x 4.5 ↔ 2.8 x 4.8}***	IEx / Ads
HEU	Heulandite	{3.1 x 7.5* + 3.6 x 4.6*} ↔ 2.8 x 4.7*	Ads
LTA	Linde Type A	4.1 x 4.1***	IEx / Dry / Ads
LTL	Linde Type L	7.1 x 7.1*	Cat
MER	Merlinoite	3.1 x 3.5* ↔ 2.7 x 3.6* ↔ {3.4 x 5.1* + 3.3 x 3.3*}	Ads
MFI	ZSM-5	{5.1 x 5.5 ↔ 5.3 x 5.6}***	Cat / Ads
MOR	Mordenite	6.5 x 7.0* ↔ {3.4 x 4.8 ↔ 2.6 x 5.7}*	Cat
MTW	ZSM-12	5.6 x 6.0*	Cat
MWW	MCM-22	⊥ 4.0 x 5.5** ⊥ 4.1 x 5.1**	Cat
RHO	Rho	3.6 x 3.6*** 3.6 x 3.6***	Cat

^a IZA code based on IUPAC rules;

^b Source, Baerlocher et al. (2007): (*) 1-, (**) 2- or (***) 3-D channel system; (↔) interconnecting channel systems; (|) no direct access from one channel system to the other; (⊥) channels interconnected at right angles. Applications: (Ads) adsorption/separation; (Cat) catalysis; (Dry) drying; (IEx) ion exchange.

II.3.3 Zeolite beta

Zeolite beta is one of the most complex materials and is of great importance in the zeolite family. The intergrowth structure of zeolite beta was first determined by Newsam et al. and Higgins et al. independently. (Tingting Lu et al.,2019). Here, we will describe the framework structure of zeolite beta and illustrate the chiral structural features of polymorph-A. A good understanding of the chiral structure is central to the synthesis and application of chiral zeolite beta.

Zeolite beta is an intergrowth of two or three polymorphs, including chiral polymorph-A, a chiral polymorph-B, and polymorph-C. Chiral polymorph-A of zeolite beta is highly desired because of its potential applications in enantioseparation and asymmetric catalysis. (Tingting Lu, et al., 2019).

Zeolite beta was first synthesized by Mobil in 1967. However, the structure of this zeolite was determined only in 1988 (Newsam et al., 1988) due to its complexity. It is reported that in zeolite beta structure, the ordered and disordered framework coexist. Zeolite beta possesses a three-dimensional pore structure consisting of perpendicular straight channels 66×67 nm which interconnections create narrow helicoidal channels of effective pore diameter 56×56 nm **Fig 7**.

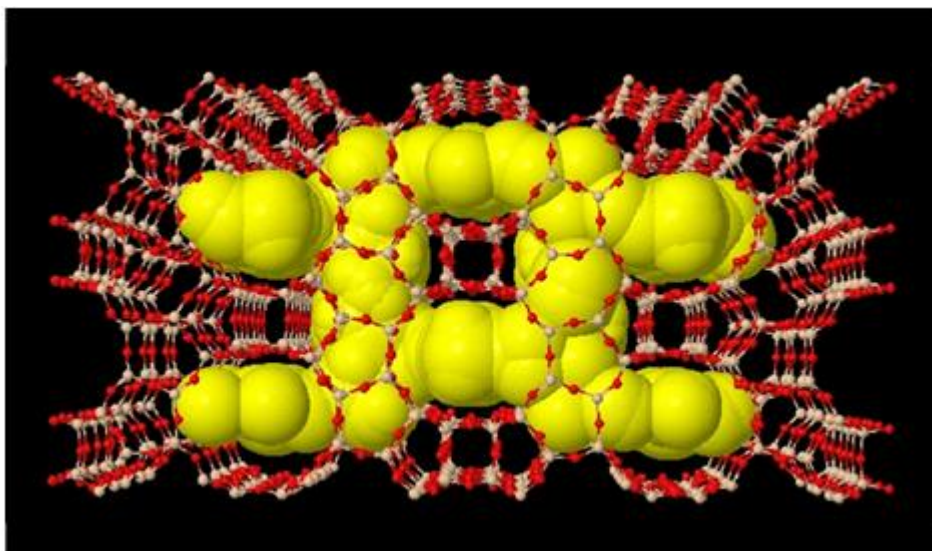


Figure 7 : Zeolite beta framework and maximum free spheres fitting inside the channels (Newsam J. M,et al.,1988).

Zeolite beta is produced in large scale for commercial applications such as catalyst and catalyst support (alkylation of aromatics, Friedel Crafts reactions, isomerization of waxes) and as a sorbent in separation of aromatics and reduction of exhaust gas emission (Guisnet and Ribeiro, 2004). The potential application of zeolite beta for the separation of branched C6 might benefit from its commercial availability (Table 3). However, there are very few published data concerning the adsorption and diffusion of alkanes in this structure, especially in commercial pellets important to set-up adsorption processes. For example, Douglas M. Ruthven (1995) in one of the reference books for diffusion in zeolites available on literature has no reference for diffusion of any compound on zeolite beta despite the importance of this zeolite in catalysis nowadays. There is also a lack of experimental data respecting the behaviour of alkane's mixtures in this material. Such information is essential for the design and development of a cyclic separation process like the Advance process separations used in the TIP and I psorb processes.

Zeolite Beta has a 3-dimensional structure (**Fig 8 a**): two channels with the pores between 76 – 64 nm. The unit cell of zeolite Beta structure is tetragonal. Zeolite Beta has been produced industrially for a long time. The laboratory synthetic procedure was created by Cambior and Pérez-Pariente (M.A. Cambior, 1991). The gel composition of Beta zeolite can be expressed by the following formula: 1.97 Na₂O: 1.00 K₂O: 12.5 (TEA)₂O: Al₂O₃: 50 SiO₂: 750 H₂O: 2.9 HCl where TEA is tetraethyl ammonium hydroxide. Beta zeolites are often used in fine chemical industries and petroleum refining by reason of its strong acidity and high thermal stability. The SEM micrograph of Na-Beta-11 and the framework structure of Beta zeolite are presented in **Fig 8 a and 8 b**, (Anna Zaykovskaya, 2018).

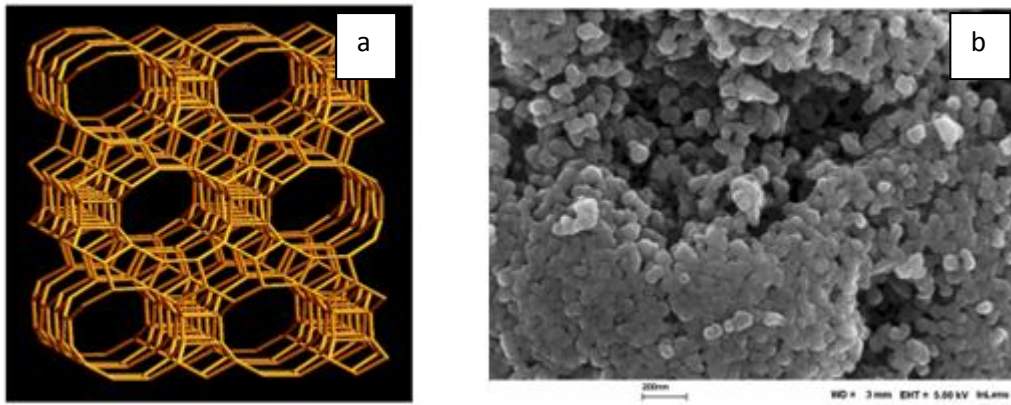


Figure 8 : Framework structure of Beta zeolite (a) and SEM micrograph of Na-Beta-11 (b). (Anna Zaykovskaya, 2018).

II.3.3.1 Synthesis

Zeolites are generally synthesized under hydrothermal conditions using hydrogels prepared from aluminate, silicate and hydroxide solution. Natural sources such as diatomite, kaolinite and other clay minerals have also been used in the synthesis of zeolites, (Garcia, G. et al., 2016; Garshasbi, V. et al., 2017). By varying the composition of synthesis solutions it is possible to obtain zeolites with different structures or the same zeolite showing different chemical compositions. (Gianetto, 2000; Anuwattana, R. et al., 2009). In summary, keeping the conditions of preparation fixed, a simple variation in the Si/Al ratio may result in different zeolites, for example, Faujasite X and sodalite ($\text{Si/Al} < 2$), mordenite and Faujasite Y ($2 < \text{Si/Al} < 5$), ZSM-5, ZSM-12 and zeolite Beta ($\text{Si/Al} > 5$), (Davis, M. E.; Lobo, R. F., 1992).

Zeolite beta (BEA) is a large pore crystalline aluminosilicate. The intergrowth of two polymorphs (A and B) related to each other, with the possibility of there being a third (C), makes up the structure of BEA. Polymorphs are constituted by a three-way system of channels delimited by rings of 12 interconnected members (Corma, A., 2003).

Among several types of natural and synthetic zeolites already reported in literature (IAZ, 2015). BEA has received special attention from the scientific community regarding its high Si/Al ratio, high surface acidity and hydrothermal stability. In addition, it shows differential catalytic properties such as activity, selectivity and resistance to deactivation over time of use, mainly in catalytic cracking

reactions, alkylation and acylation of aromatic hydrocarbons, and alkane hydroisomerization, among others already reported (Yaqiong Qiu et al., 2007).

Research on variation in the Si/Al ratio, time and temperature of zeolite synthesis has shown that modification of these parameters is able to change the physical properties of zeolites (Ding, L. et al., 2007; Maia, A. Á. B. et al, 2015). Variation in temperature and crystallization time guided the formation of the most stable phase for zeolite synthesis, or contributed to the growth of different crystalline structures(Davis, M. E.; Lobo, R. F,1992; Ding, L. et al., 2007).

Table 4 : Conditions employed in the synthesis of zeolites (Nascimento, A. R. et al., 2017).

Si/Al ratio	Crystallization time (Days)	Crystallization temperature(°C)
8	2	135
8	2	170
8	4	135
8	4	170
14	3	152
14	3	152
14	3	152
20	2	135
20	2	170
20	4	135
20	4	170

III. CHROMATOGRAPHY FRONTAL

Forward chromatography is a type of chromatography in which the sample is fed continuously into the column. The sample components migrate through the column at different velocities and eventually and eventually break off at various fronts. Only the least trapped compound exits the column pure and can therefore be all other components exit the column as mixed regions. The chromatogram resulting from a frontal chromatography experiment is called a breakthrough curve, breakthrough curve or «frontal gram».

The exact shape of a breakthrough curve is determined primarily by the underlying functional form of the equilibrium isotherm, but secondary factors such as diffusion and mass transfer kinetics also have an influence. Column capacity is a key parameter in forward chromatography as it determines when the column is saturated with the adsorbate and therefore cannot absorb more molecules. Adsorb more molecules. From that moment on, the mixture flows through the column with the initial composition. (Nicolau, 2008)

III.1 Adsorption in Fixed Bed

Fixed bed adsorption represents a widely used technique in adsorption processes. It can be used in separation processes at the industrial level, as well as to estimate parameters at the laboratory scale.

Fixed bed adsorption is often used for gas purification and bulk separation.

Consider a fluid stream containing an adsorbable component passing through a fixed bed of adsorbent, and given the following assumptions:

1. Reduced internal and external mass transfer resistance.
2. Piston flow.
3. Initially the adsorbent is free of adsorbate.
4. The adsorption isotherm starts at the source.

The adsorption equilibrium between the fluid and the adsorbent is then instantaneously reached, resulting a shock wave or more commonly called, stoichiometric front **Fig 9**, (Nicolau, 2008)

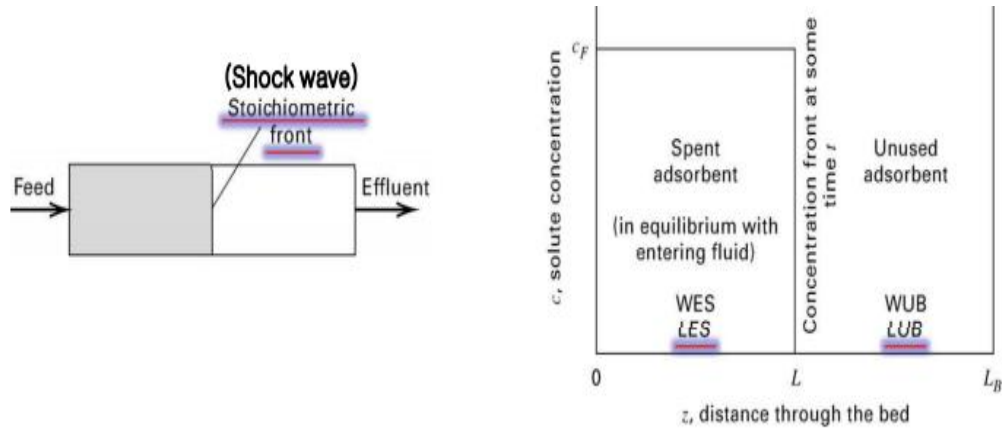


Figure 9 : Example of a stoichiometric front for ideal fixed-bed adsorption. (Matiwaza Ncube, Yuehong Su, 2012).

Upstream of the shock front the adsorbent is saturated with the adsorbate and the solute concentration in the fluid corresponds to the inlet concentration to the column (feed concentration). In the upstream region, the adsorbent is "depleted" or saturated, while downstream of the stoichiometric front and at the exit of the column, the solute concentration in the fluid phase is still zero, and the adsorbent remains free of adsorbate. (Bárcia, et al., 2003).

After a certain time, called stoichiometric time, the stoichiometric front reaches the top of the bed, increasing the concentration of the adsorbate. The adsorbent is still free of adsorbate and the adsorbent is still free of adsorbate, (Nicolau, 2008).

Fig 10 shows a schematic of a typical Breakthrough curve that is obtained using a fixed bed.

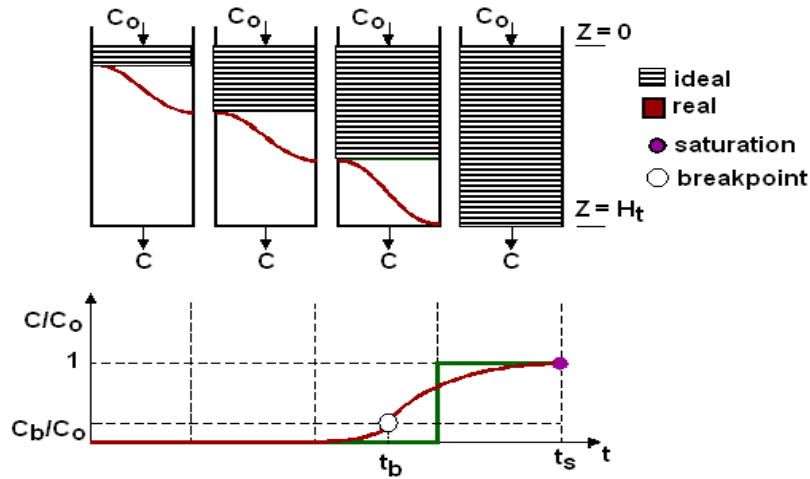


Figure 10 : Breakthrough curve for the sorption process in fixed beds C_o is the concentration of the inlet solution, C_b is the concentration of the breakthrough, t_b is the break point time and t_s is the saturation time,(Barros M. A. S et al., 2013).

When the solute-rich fluid comes in contact with the bed containing the adsorbent, the fluid phase is adsorbed. Solid material immediately adsorbs the adsorbate until equilibrium is reached with the Saturation Point. The adsorption action continues until the introduced feed solution saturates the entire bed.

The curvilinear behavior of the breakthrough curve delineates a region of the bed in which adsorption is occurring. The saturation point indicates the complete depletion of the column, i.e., it is reached when the column outlet concentration is equal to the input concentration ($C/C_o=1$).

An important factor in fixed-bed adsorption is the size and shape of the adsorbent particles. The particles when packed together, form a bed with an average interparticle porosity called ϵ_b , and is defined as:

$$\epsilon_b = \frac{\text{volume of voids between the particles}}{\text{total bed volume}} \quad (7)$$

In a poorly packed bed, ϵ_b can vary considerably in different parts of the column, leading to uneven flow distribution or the formation of "by-pass" preference channels ("channeling effects"), which leads to a decrease in separation (Daniela, 2009).

III.1 Breakthrough curves measurements

During the breakthrough experiments, the solute adsorbs onto the pores of the adsorbent until the bed becomes saturated.

From that moment on, the detector attached to the column outlet starts to register a signal regarding the solute concentration in the outlet stream. The signal increases relatively sharply until a new equilibrium state is reached, which corresponds to the instant when the concentration at the column outlet equals the concentration in the column feed. From this record, you get a chromatogram similar to the one in **Fig 11**, where the dashed area represents in practice the amount of solute adsorbed (Bárcia, et al., 2003).

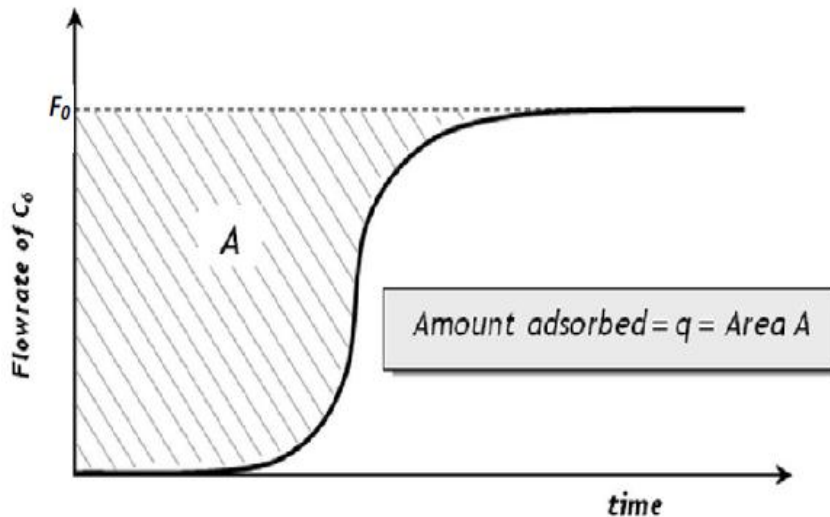


Figure 11 : Schematic representation of an experimental breakthrough curve and the adsorbed amount (q_0). (Bárcia, et al.2006).

In this type of experiment it is necessary to establish a relationship between the signal collected by the detector and the effective concentration by performing a calibration. Due to the large number of experimental points collected during a breakthrough, the amount adsorbed can be accurately determined using a simple numerical integration method such as the trapezoid method (Bárcia, et al., 2003).

IV. EXPERIMENTAL SECTION

IV.1 Characterization of Xylene and Ethylbenzene Isomers

Xylene is a generic term for a group of three aromatic hydrocarbons derived primarily from benzene and of chemical formula $C_6H_4(CH_3)_2$. According to the position of the methyl groups present on the benzene ring of these hydrocarbons, it is named o-xylene (1, 2-dimethylbenzene), m-xylene (1,3-dimethylbenzene), and p-xylene (1,4-dimethylbenzene). These are therefore referred to as xylene isomers.

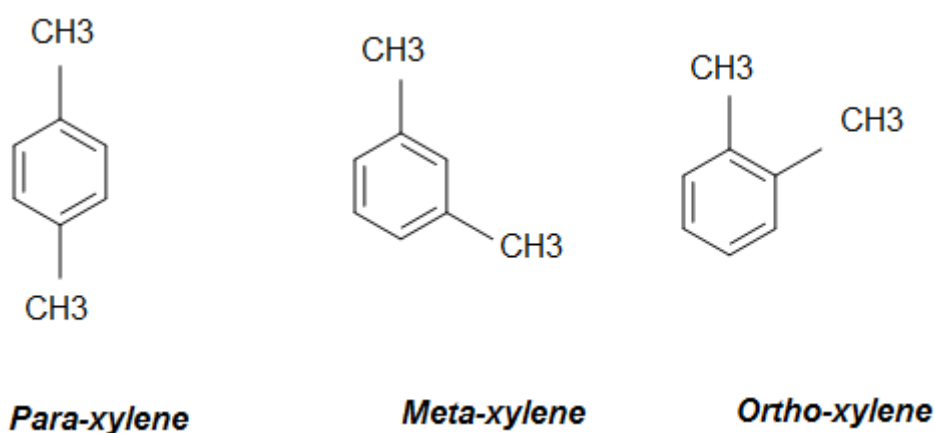
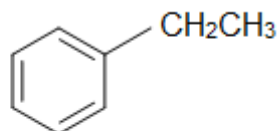


Figure 12: Representation of xylene isomers.

Xylene is a colorless liquid, insoluble in water and miscible with ethanol, ether and other organic solvents, odor characteristic, harmful and flammable, and its commercial solution results from a mixture of its isomers, ethylbenzene and other aromatic hydrocarbons.

Ethylbenzene is, like xylene, an aromatic hydrocarbon with the chemical formula $C_6H_5CH_2CH_3$. While the xylene isomers have two methyl groups attached to the benzene ring, ethylbenzene has one ethyl group, as shown in **Fig 13**.



Ethylbenzene

Figure 13 : Representation of ethylbenzene.

The physicochemical properties of ethylbenzene are identical to that of xylene.

The para-xylene and ortho-xylene isomers as well as the ethylbenzene used during the study were purchased from Merck ($\geq 99\%$). The meta-xylene isomer was purchased from Alfa Aesar ($\geq 99\%$).

The fact that they have different configurations, notably at the substituents attached to the benzenes ring, these compounds have different kinetic diameters, as shown in **Table 5**.

Table 5: Kinetic diameters of the compounds present in the system (Nicolau, 2008).

Compound	kinetic diameter, d_k (nm)
Para-Xylene	0.67
Meta-Xylene	0.71
Ortho-Xylene	0.74
Ethylbenzene	0.67

IV.2 Characterization of the zeolite BETA under study

The zeolite beta was characterized and analyzed by five methods are

1. Scanning electron microscopy

The commercial samples of zeolite beta in the H^+ form used in this study were supplied by Süd-Chemie AG in both powder and pellet form under the reference H⁺BEA

150. The $\text{SiO}_2/\text{Al}_2\text{O}_3$ ratio is 150. The 1/16 cylindrical extrudate has an average length of 4 mm **Fig 14 (A)**.

The surfaces and cross sections of the pellets were examined by scanning electron microscopy (SEM) performed at CEMUP (University of Porto) to determine the morphology, size and homogeneity of the crystals. Panel's b-d of Figure 15 show that the crystals size in the extrudate is between 0.2 to 0.4 μm . Moreover, panel c of Figure15 also shows that crystals are smashed at the surface of the pellet probably due to the nature of the extrusion process.

According to the supplier, the inert silica used as binding agent represents 30 wt% of the pellets; this value was experimentally confirmed by comparison of the nHEX adsorption in both powder and pellet form.

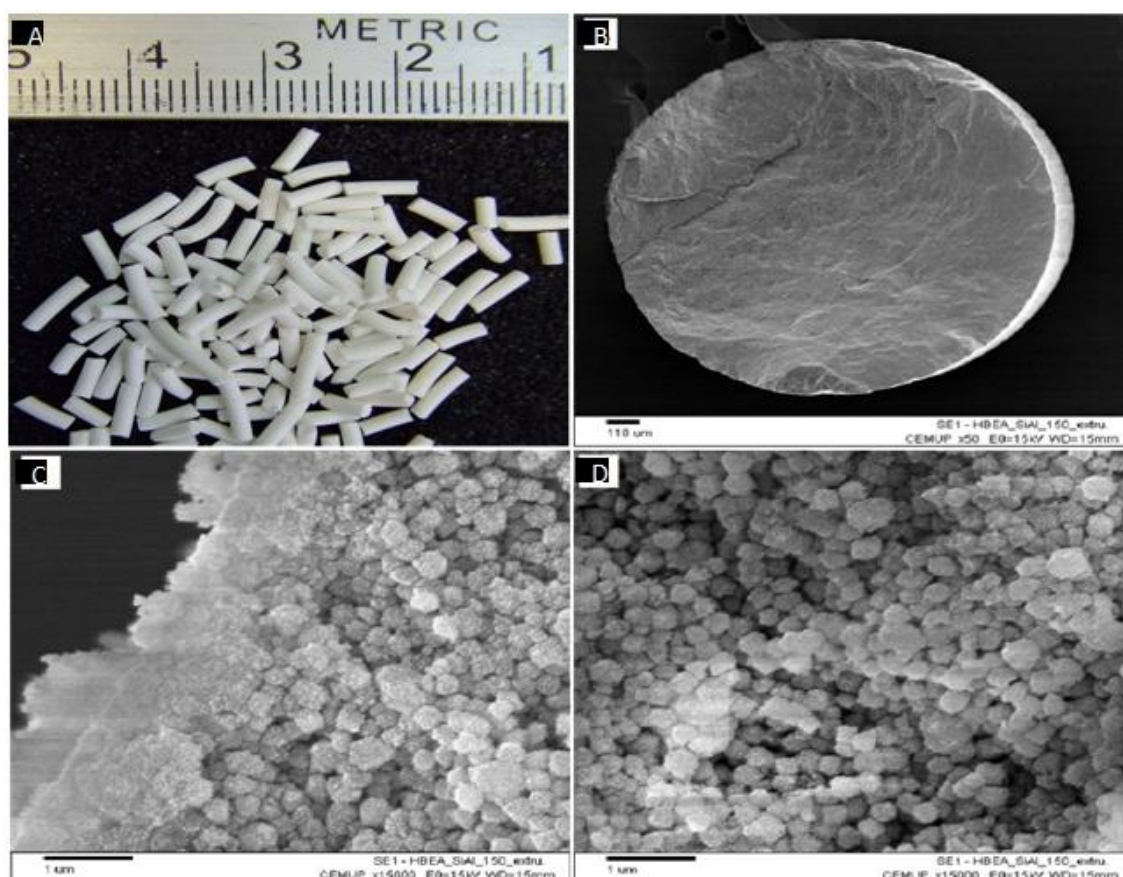


Figure 14 : (A) Zeolite beta pellets provided by Süd-Chemie AG ($\text{Si}/\text{Al}=75$). Scanning electron micrographs (SEM): (B) top view of the pellet (50 \times); (C) and (D) different view of transversal cut (15.000 \times). (Bárcia, et al., 2006).

2. Stereoscopy

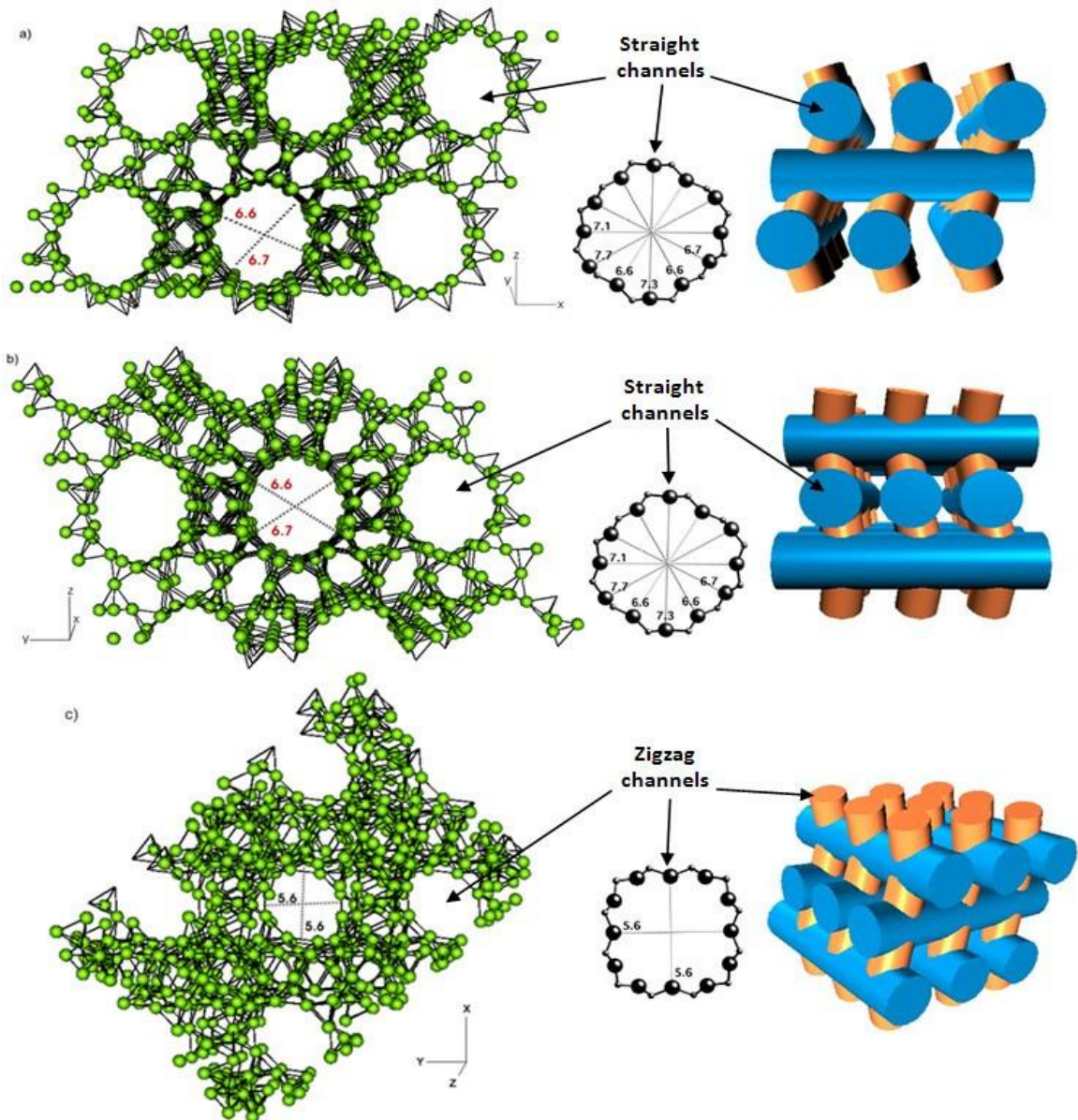


Figure 15 : Stereographic drawings and perspectives views of zeolite beta viewed along axis (a) [010], (b) [100] and (c) [001], (Bárcia, et al.2006).

The 12-MR pores of straight and zigzag channels were also shown for a good visualization of its structure. In the stereographic drawings the spheres represent the oxygen atoms and the tetrahedron which surround the tetrahedrally coordinated Si or Al T-atoms. The stereographic drawings were obtained from <http://www.iza-structure.org/databases/>. In the right side, the perspective views show the pore network of zeolite beta containing straight (blue) and zigzag (orange) channels. This

representation facilitates the visualization of the intersections between the straight and zigzag channels.

3. X-ray diffraction

The commercial powder of zeolite beta used to prepare the pellets was analyzed by X-ray diffraction (XRD) performed at the Department of Materials Science and Engineering of the Delft University of Technology (The Netherland) using a Bruker-AXS D5005 with Cu K radiation. **Fig 16** shows the corresponding XRD pattern where it can be seen that the diffraction peaks observed at $2\theta = 7.7^\circ$ and $2\theta = 22.5^\circ$ for all samples are in agreement with the more intense peaks of the reference simulated pattern for the BEA structure obtained from the Database of Zeolite Structures (<http://www.iza-structure.org>).

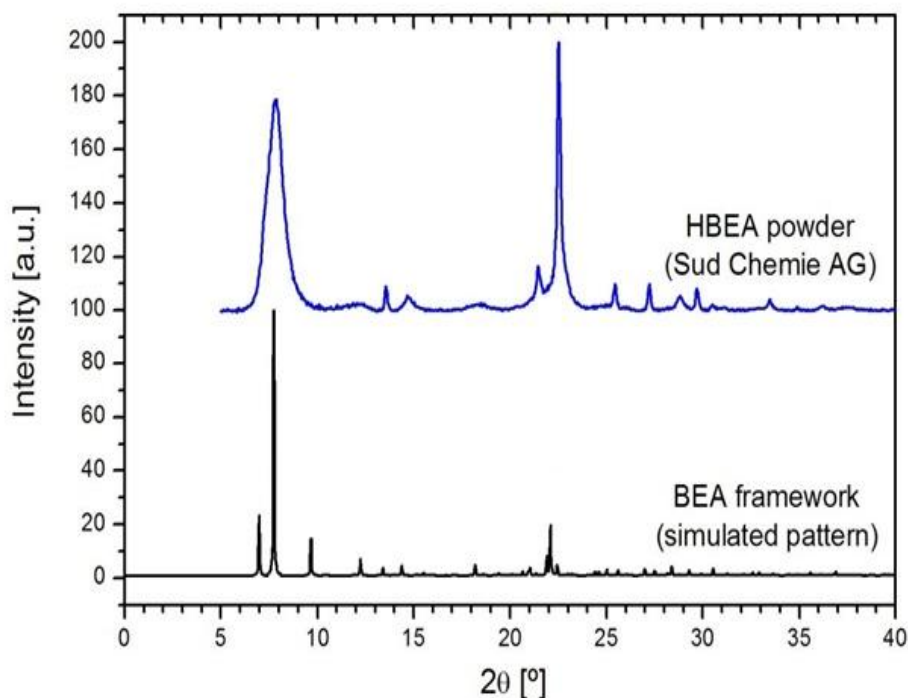


Figure 16 : XRD pattern of the commercial zeolite beta powder compared with the reference simulated pattern (Bárca, et al.2006).

4. N₂ Adsorption

N₂ adsorption at 77 K was measured on a Micrometrics ASAP 2000 at LABGRAN (Coimbra, Portugal). The pore size distribution in the commercial zeolite beta was obtained using the Barrett-Joiner-Halenda (BJH) method **Fig 17**. It can be seen from this figure that these material contains large pore volume in the transition region between mesopores and macropore with a mean pore size of about 75 nm. A smaller peak falling in the range of 3–4 nm also indicates the existence of smaller mesopores.

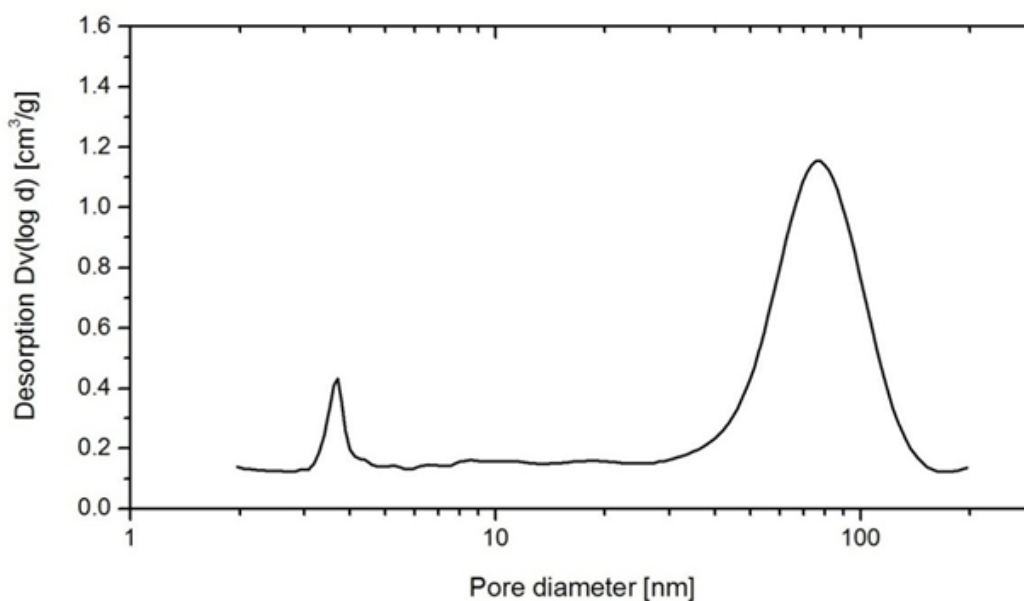


Figure 17 : Pore size distribution obtained from the N₂ desorption data using the BJH formalism, in the Süd-Chemie AG zeolite beta sample. (Bárcia,et al.2006).

5. The mercury porosimetry

The mercury porosimetry was performed by LABGRAN (Coimbra, Portugal) with a Micrometrics Poresizer 9320, which operate between 0.5 and 30 000 psia. Mercury porosimetry results for the pellets, and data relative to the zeolite crystals are reported in **Table 6**.

Table 6 : Physical properties of zeolite beta crystals, mercury porosimetry data and N₂ adsorption data of pellets (Bárcia, et al.2006).

Physical proprieties of crystals	
Si/Al ratio (mol/mol)	75
Particle dimensions (μm) ^a	0.25-0.40
Oxygen's in window	12
Channel size (nm)	0.66×0.67↔ 0.56×0.56
Mercury porosimetry data	
Intrusion volume (≈2–30 000 psia) (cm ³ /g)	0.14
Pellet density, ρ _p (g/cm ³)	1.18
Porosity (Hg probe), ε _p	0.17
N2 adsorption data	
SBET (m ² /g)	447.8
Pore volume in the range 20–2000 Å (cm ³ /g)	0.32
Porosity (N ₂ probe), ε _p	0.40
Average mesopore diameter (Å)	35
Average macropore diameter (Å)	750
^a Determined by SEM	

IV.2.1 Activation and Preparation of the Zeolite BETA for Packing the Column

Before starting any kind of experiment with the zeolite beta, it is necessary to remove the adsorbed water. To remove water from zeolite beta, this material was placed at 150°C over night (approximately 12 hours) in a vacuum oven.

IV.3 Experimental Procedure

IV.3.1 Adsorption Equilibrium Apparatus

The equilibrium adsorption data was measured in an apparatus developed at the CIMO (Centro de Investigação de Montanha) to measure single component breakthrough curves in the vapor phase in a fixed bed (dynamic system). **Fig 18** shows its schematic diagram. The experimental setup consists of two main sections: (i) gas preparation and (ii) adsorption.

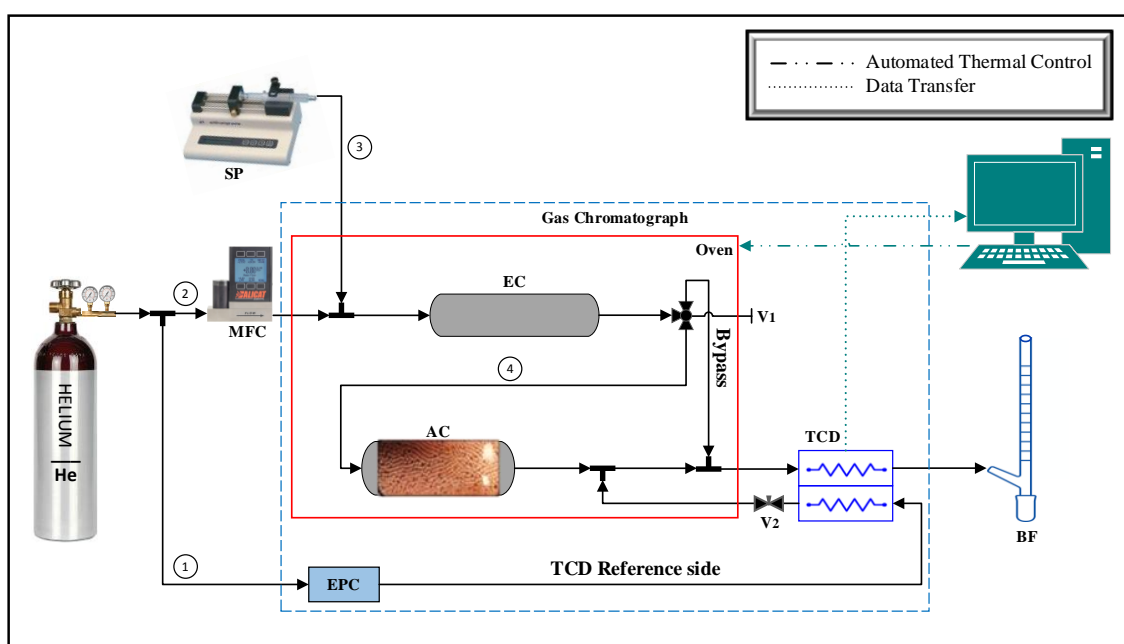


Figure 18 : Schematic diagram of the adsorption equilibrium apparatus used to measure adsorption equilibrium data: (MFC) mass flow controller; (SP) syringe pump; (AC) adsorption column; (EC) expansion column; (EPC) electronic pressure control; (TCD) thermal conductivity detector; (V1) 3-way ball valve; (V2) flow metering valve, (BF) bubble flowmeter, and (①②③④) streams.

In the gas preparation section, the carrier gas helium (ALPHAGAZ 2, 99.9999 %, Air Liquide) and the xylene isomer are introduced into the system. Helium is used as a carrier gas due to its inertness and is introduced in the system in two different streams: the first line (1) passes through an electronic pressure controller (EPC) and goes directly to the reference side of the Thermal Conductivity Detector (TCD); and the second line (2) through a mass flow controller (MFC, MC-100SCCM-D/5M, Alicat Scientific). The hydrocarbon stream, line (3), is continuously introduced (in liquid phase) with a syringe

pump (SP, SP100i, World Precision Instruments). A gastight syringe Luer lock was used (5MDF-LL-GT, Scientific Glass Engineering). Both lines (2) and (3) goes to the gas chromatograph oven, where they are mixed and run into the expansion column (EC, stainless steel with 100 mm of length and 8 mm in internal diameter) for the complete vaporization of the mixture. Then, the gas mixture runs to a 3-way ball valve (V1, SS-41GXS1, Swagelok), initially directed to the bypass line. The column bypass is incorporated to check, before starting any experiment, if the paraffin vaporization is stable, i.e., if it shows a constant concentration in the TCD. It can be seen that the helium flowing in the reference side of TCD is used to dilute the signal of the vaporized mixture, being its flowrate adjusted by a flow metering valve (V2, SS-SS2, Swagelok). Both valves (V1) and (V2) operate manually. At the end of the system (output of TCD), a manual bubble flowmeter (BF, 10CC EA, Supelco) is coupled to check and calibrate all gas flowrates.

Once the vaporized mixture concentration reaches a constant signal in the TCD detector, the experiment can be started (adsorption section). Therefore, the valve (V1) is actuated, allowing the mixture (carrier gas plus xylene) flow through line (4) to run into the adsorption column, which is filled with the adsorbent material. Over the entire experiment, the output stream of the packed column is constantly monitored by the thermal conductivity detector and the signal recorded in a computer.

When the experiment finishes, i.e., the saturation state is reached with no change in the composition at the outlet of the column, giving rise to the breakthrough curve, the xylene injection by the syringe pump is cut, and only helium gas flow through the system to clean the column (desorption of the previously adsorbed xylene isomer). After the column regeneration, another experiment can be performed. Before the first RUN, the packed column was activated for 12 h at 573 K under a pure helium flow in a vacuum atmosphere.

The gas chromatograph used (SRI 310C, SRI Instruments) to build the experimental setup is equipped with a forced convection oven to keep the column near isothermal conditions. The oven temperature and the TCD signal are controlled and recorded, respectively, by the data acquisition software PeakSimple (SRI Instruments), a chromatography data system with an intuitive and user-friendly interface.

Fig 19 (panels a and b) show a realistic view of the experimental apparatus.

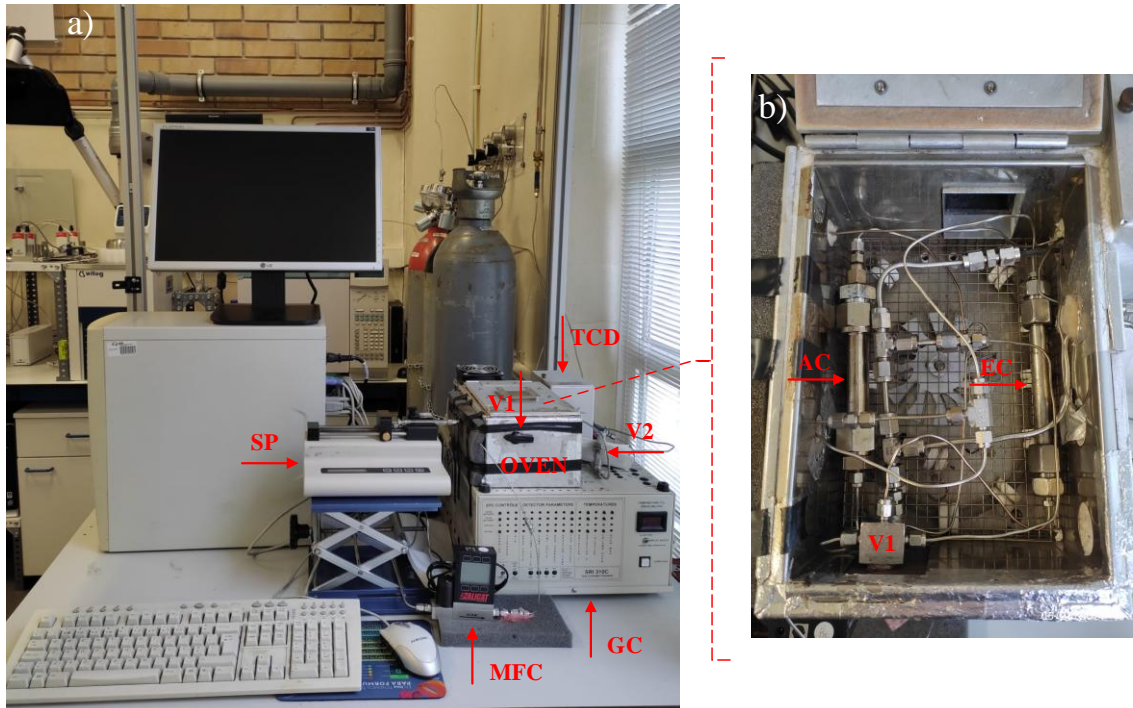


Figure 19 : Real view of the adsorption equilibrium apparatus: a) detailed view of the components system, and b) close-up inside the chromatograph oven.

IV.3.2 Experimental Procedure for Breakthrough Measurements

The experimental procedure to obtain single component breakthrough curves consists of continuously measuring the concentration profile of the xylene isomer as a function of time at the outlet of the adsorption column. For that, the packed bed is saturated by introducing, at the inlet, the feed containing the xylene isomer with a known composition and molar flux in a helium stream at a constant total hydrocarbon pressure and temperature. For each experimental breakthrough curve, the amount adsorbed in the material is obtained by integrating the molar rate history of the reached breakthrough curve as follows:

$$q_{exp} = \frac{1}{m_{ads}} \left(F_0 t_n - \int_0^{t_\infty} F dt - \varepsilon_b V_c C_0 \right) \quad (8)$$

where m_{ads} (g_{ads}) is the adsorbent mass in the column, F_0 (mol /cm³) is the feed molar flow rate of xylene isomer, F (mol/cm³) is the molar flow rate of xylene isomer in the bulk gas phase, t_{∞} (min) is the saturation bed time, ε_b is the bed porosity, V_c (cm³) is the column adsorption volume and C_0 (g/cm³) is the feed gas-phase concentration at the inlet of the fixed bed. The term $\varepsilon_b V_c C_0 / m_{ads}$ represents the adsorbed amount of sorbate gas in the column void space.

V. RESULTS AND DISCUSSION

V.1 Breakthrough Curves

A series of breakthrough tests were conducted to determine the amount adsorbed for a particular pressure in order to set-up the adsorption isotherms of the xylene isomers.

In both experiments, the syringe used in all the experiments is a Hamilton 5.0 mL syringe; being carried out experiments at the temperatures of 125, 150 and 175 °C, until a partial pressure of 0.100 bar.

Table 7 provides the full details on the experiments, namely: the studied compound, partial pressure, temperature, flowrate of the aromatic product, adsorbed amount for each experiment.

In all experiments, it is important to remember that the mass of BEA packed on the column was the same and equal to 480 mg of BEA. By numerical integration of the curve with the Trapezoidal process, the amount of adsorbed was determined in the way described in section III.1.

Table 7: Operating conditions for fixed bed experiments performed with pure aromatic components (C_8H_{10}) and respective adsorbed amounts.

Temperature (°C)	Partial pressure (bar)	flow of He (ml/min)	flow of C_8H_{10} (μ mol/min)	Adsorbed quantity (g/100gads)	Run
Para – Xylene					
125	0.1	57.93	259.7	0.7714	1
	0.075	59.54	194.7	0.7075	2
	0.05	61.15	129.8	0.6151	3
	0.025	62.76	64.92	0.5304	4
150	0.1	54.51	244.3	0.6213	5
	0.075	56.02	183.2	0.5301	6
	0.05	57.53	122.2	0.4744	7
	0.025	59.05	61.08	0.4467	8
175	0.1	55.75	230.7	0.4873	9
	0.075	54.33	173	0.4040	10
	0.05	52.90	115.3	0.3741	11
	0.025	51.47	576.7	0.3358	12
Meta – Xylene					
125	0.1	57.93	259.7	0.7280	13
	0.075	59.54	194.7	0.7152	14
	0.05	61.15	129.8	0.6569	15
	0.025	62.76	64.92	0.5380	16
150	0.1	54.51	244.3	0.5302	17
	0.075	56.02	183.2	0.4656	18
	0.05	57.53	122.2	0.4252	19
	0.025	59.05	61.08	0.3716	20
175	0.1	55.75	230.7	0.3689	21
	0.075	54.33	173	0.3077	22
	0.05	52.90	115.3	0.2995	23
	0.025	51.47	576.7	0.2442	24

Table 7 : continuation

Ortho – Xylene					
125	0.1	57.93	259.7	0.8073	25
	0.075	59.54	194.7	0.7593	26
	0.05	61.15	129.8	0.6410	27
	0.025	62.76	64.92	0.5563	28
150	0.1	54.51	244.3	0.5101	29
	0.075	56.02	183.2	0.4800	30
	0.05	57.53	122.2	0.4122	31
	0.025	59.05	61.08	0.3416	32
175	0.1	55.75	230.7	0.3856	33
	0.075	54.33	173	0.3486	34
	0.05	52.90	115.3	0.2990	35
	0.025	51.47	576.7	0.2496	36
Ethylbenzene					
125	0.1	57.93	259.7	0.8174	37
	0.075	59.54	194.7	0.7303	38
	0.05	61.15	129.8	0.6853	39
	0.025	62.76	64.92	0.5805	40
150	0.1	54.51	244.3	0.4510	41
	0.075	56.02	183.2	0.4187	42
	0.05	57.53	122.2	0.5490	43
	0.025	59.05	61.08	0.5780	44
175	0.1	55.75	230.7	0.4371	45
	0.075	54.33	173	0.3228	46
	0.05	52.90	115.3	0.2932	47
	0.025	51.47	576.7	0.2506	48

V.2 Influence of Temperature on the Breakthrough Curves of Pure Components

In **Fig 23** the influence of temperature on the single-component breakthrough curves at a pressure of 0.100 bar is shown. As expected, under the same operating conditions, the increase in temperature causes a faster saturation of the adsorbent, which means a smaller amount adsorbed. Note that Figure is for P-X, but the same behavior is evident in the breakthroughs for the other compounds.

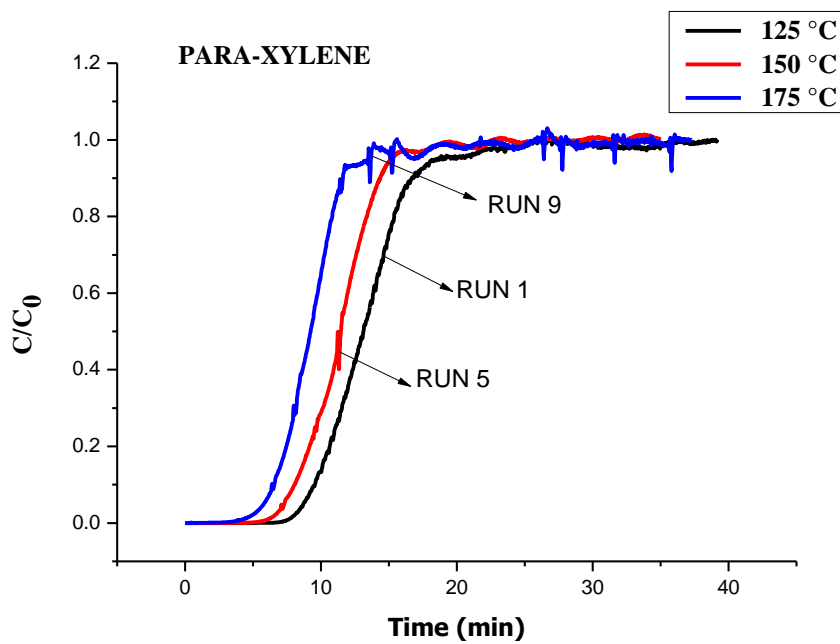


Figure 20 : Influence of temperature on breakthrough curves for p-xylene at the partial pressure of 0.100 bar

V.3 Isotherms of Adsorption

Adsorption of a gas by a porous material is described quantitatively by an adsorption isotherm, the amount of gas adsorbed by the material at a fixed temperature as a function of pressure. Porous materials are most frequently characterized in terms of pore sizes derived from gas sorption data, and IUPAC conventions have been proposed for classifying pore sizes and gas sorption isotherms that reflect the relationship between porosity and sorption (Zeid A. ALothman, 2012).

The six types of isotherm (IUPAC classification) are characteristic of adsorbents that are microporous (type I), nonporous or macroporous (types II, III, and VI), or mesoporous (types IV and V), (Shields, J.E et al.,2004).

From the series of breakthrough curves shown in **Table 7** the adsorption isotherms were collected for each compound.

V. 3.1 Adsorption Isotherms

Figs 21, 22, 23, and 24 show the adsorption isotherms of the four aromatic compounds.

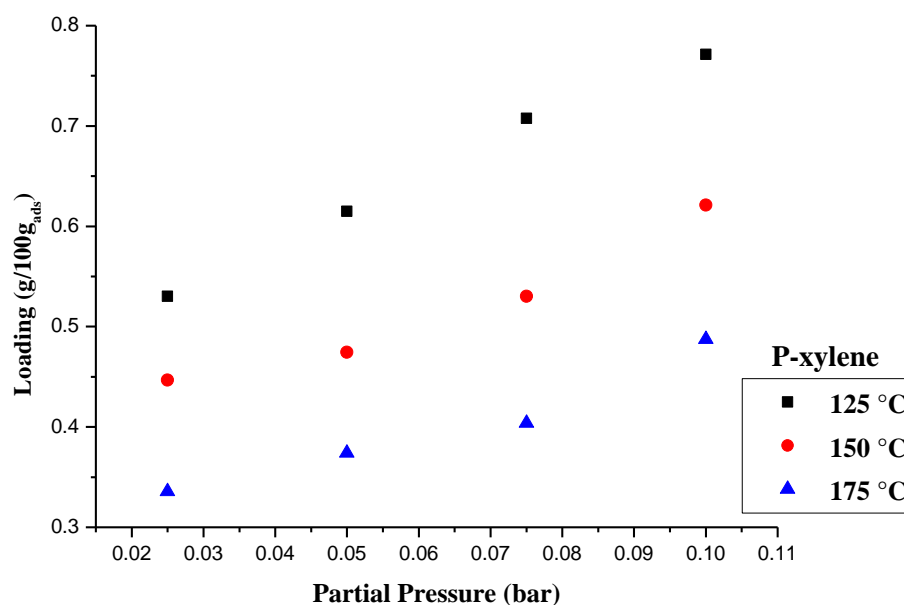


Figure 21 : Adsorption isotherms of p-xylene at three different temperatures.

If one looks to the adsorption isotherms below, it can be concluded that they are classified as IUPAC category I.

Reversible Type I isotherms are given by microporous solids having relatively small external surfaces (e.g., some activated carbons, molecular sieve zeolites and certain porous oxides). A Type I isotherm is concave to the partial pressure axis and the amount adsorbed approaches a limiting value. This limiting uptake is governed by the accessible micropore volume rather than by the internal surface area. A steep uptake at very low partial pressure is due to enhanced adsorbent-adsorptive interactions in narrow micropores (micropores of molecular dimensions), resulting in micropore filling at very low partial pressure, (Wenming Hao et al, 2018).

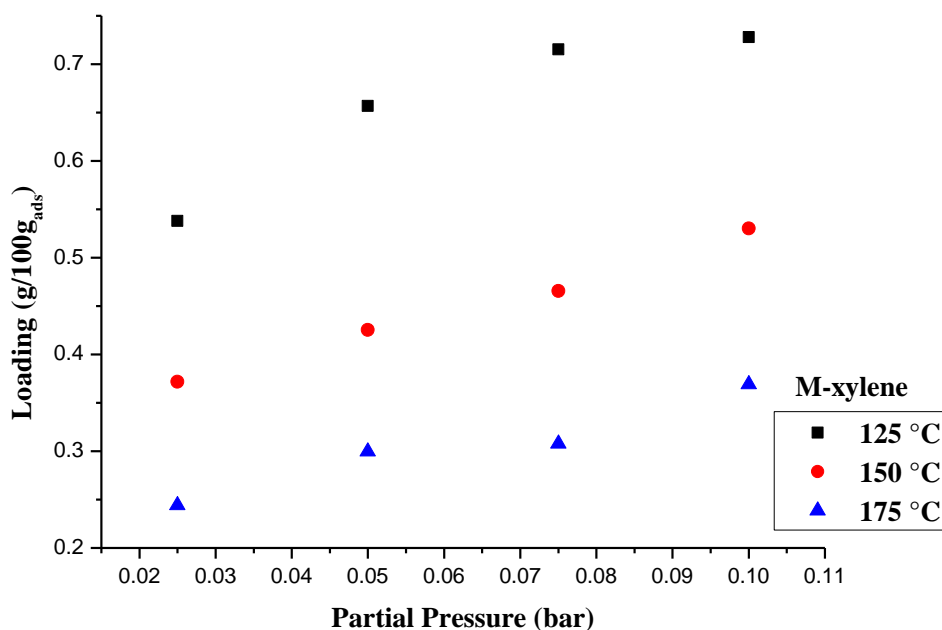


Figure 22 : Adsorption isotherms of pure M-xylene components at three different temperatures.

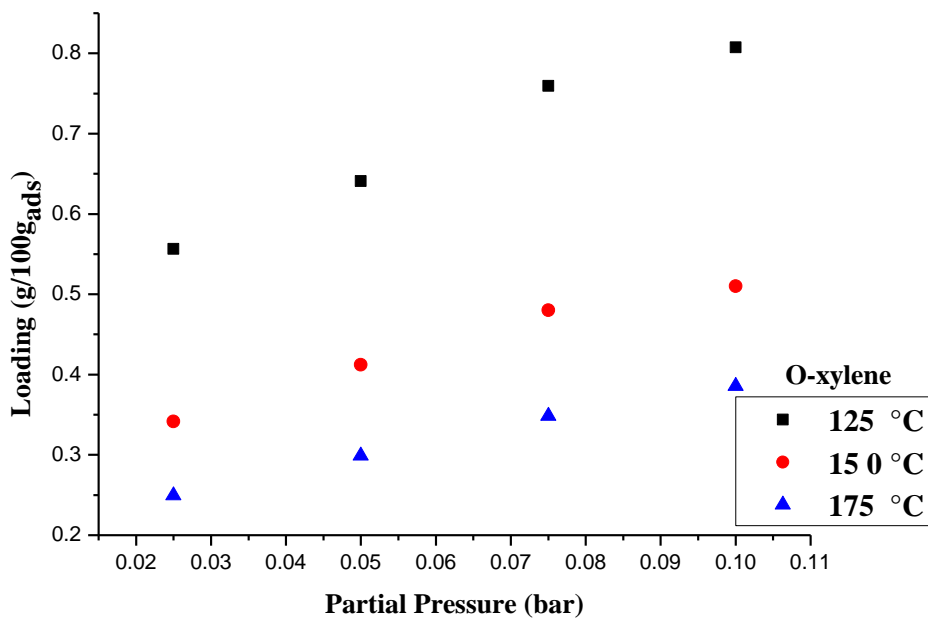


Figure 23 : Adsorption isotherms of pure O-xylene components at three different temperatures.

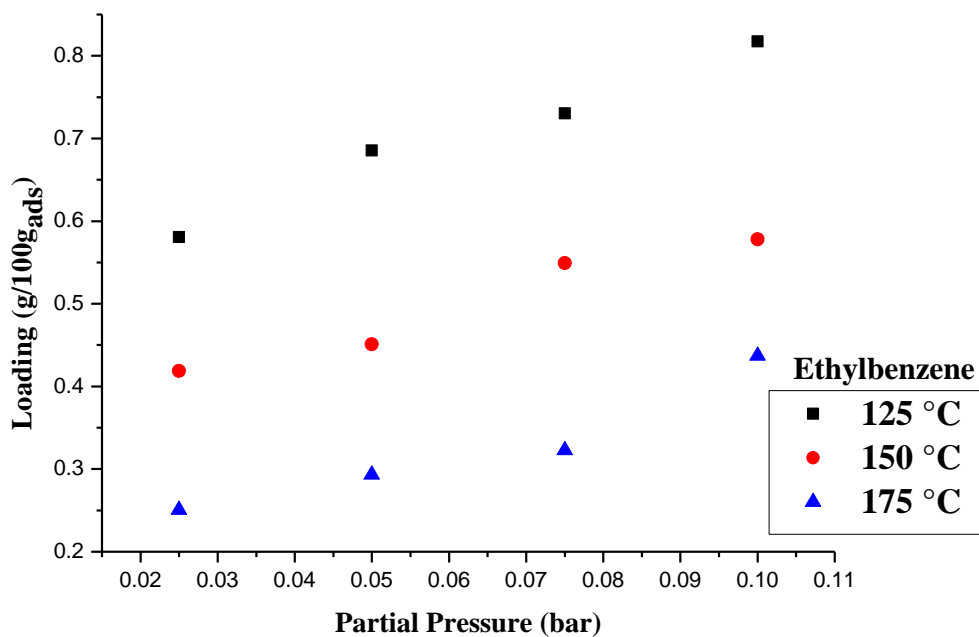


Figure 24 : Adsorption isotherms of pure Ethylbenzene components at three different temperatures.

V. 4 Comparison of Adsorption Isotherms

By observing **Figs 25, 26** and **27** it can be seen that the loading are increasing with the increase of the partial pressure. Also it can conclude that the selectivity is seen to be very low except for the para-xylene it seems that it has a high one at 175 °C. The highest adsorption capacity is nearly 0.8 g/100 g_{ads}, and it has been obtained at 125 °C for the ethylbenzene.

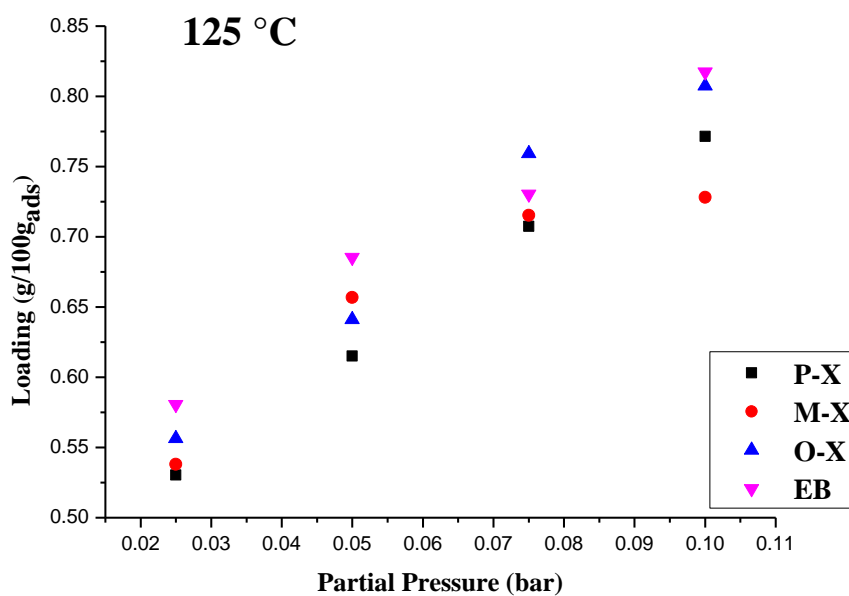


Figure 25 : Comparison of the pure component isotherms of the four aromatic compounds at 125°C.

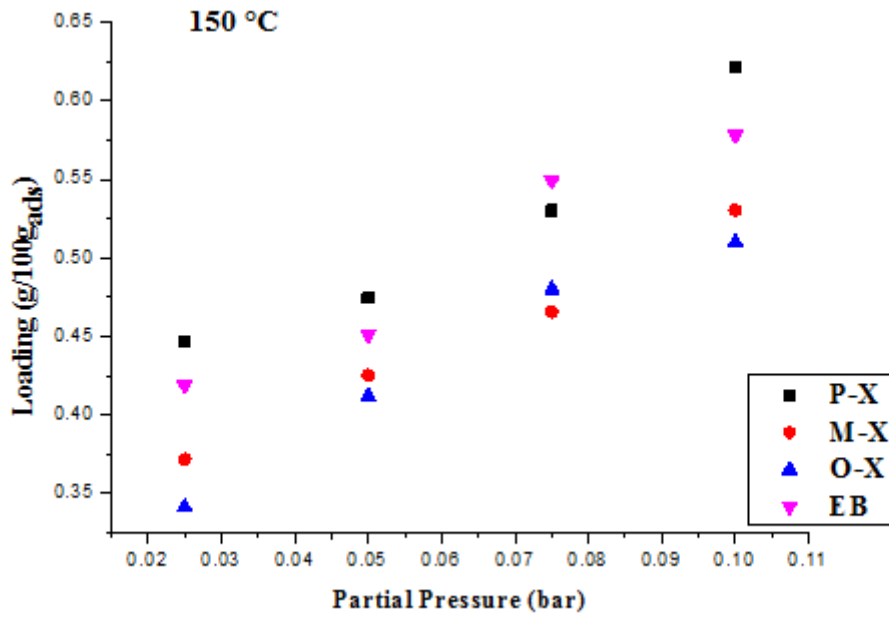


Figure 26 : Comparison of the pure component isotherms of the four aromatic compounds at 150°C.

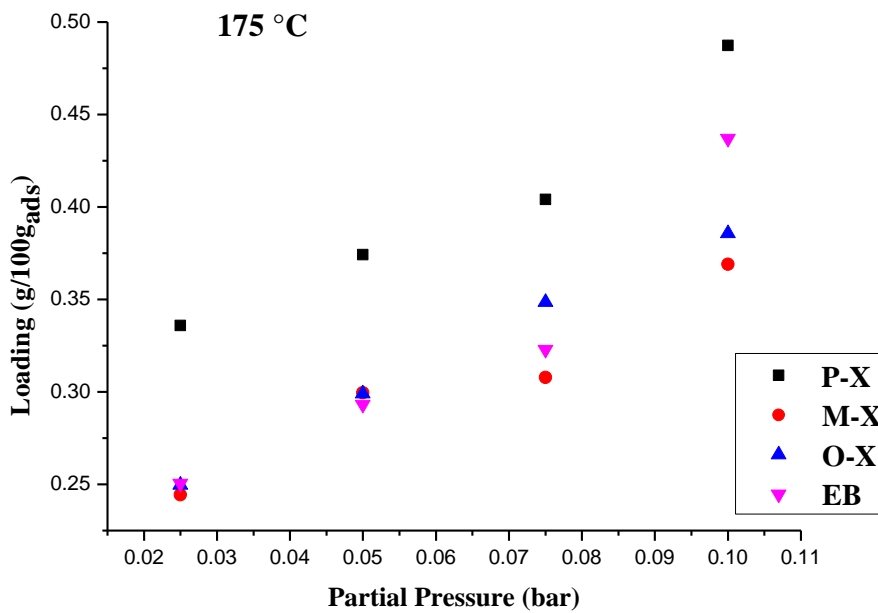


Figure 27 : Comparison of the pure component isotherms of the four aromatic compounds at 175°C.

V. 5 Modeling of Experimental Data

V. 5.1 Modeling of Isotherm data

Zeolite BETA has two distinct channels in its structure, zigzag and straight channels with similar apertures of the kinetic diameters of xylene isomers, in which the xylene isomers are adsorbed on both. So the Langmuir and dual site Langmuir adsorption equilibrium models were used to fit the data. This was performed by a non-linear Excel optimizer (solver).

Table 8 displays the results obtained. The fit of the isothermal model PX, MX, OX and EB respectively are shown in **Figs 28, 29, 30** and **31**.

The DSL fits very well the data, but the Langmuir model does not fit experimental data well. it had been used the curves of the model which best fitted our isotherms.

Table 8 : Parameters obtained for the isotherm models (Langmuir, DSL) regarding the adsorption of xylene isomers and ethylbenzene on Zeolite beta and the mean absolute deviations between the models and the experimental data.

Compounds	Para-Xylene		Meta-Xylene		Ortho-Xylene		Ethylbenzene	
	Lang.	DSL	Lang.	DSL	Lang.	DSL	Lang.	DSL
q_s (g/100g _{ads})	0.7812	-	0.8682	-	0.9557	-	0.9350	-
q_s^c (g/100g _{ads})	-	0.5545	-	0.2562	-	0.2586	-	0.2628
q_s^j (g/100g _{ads})	-	1.0226	-	1.3569	-	0.6281	-	1.4673
$-\Delta H$ (kJ/mol)	47.473	-	47.473	-	47.473	-	47.473	-
$-\Delta H_1$ (kJ/mol)	-	31.18280	-	3.118	-	31.188	-	3.118
$-\Delta H_2$ (kJ/mol)	-	31.202	-	3.121	-	31.113	-	3.113
b (k Pa ⁻¹)	0.05378	-	0.0286	-	0.0239	-	0.029	-
b^c (k Pa ⁻¹)	-	9.1	-	0.1283	-	10.3387	-	10.3381
b^j (k Pa ⁻¹)	-	1.9	-	0.0004	-	0.0009	-	0.0004

Para-xylene

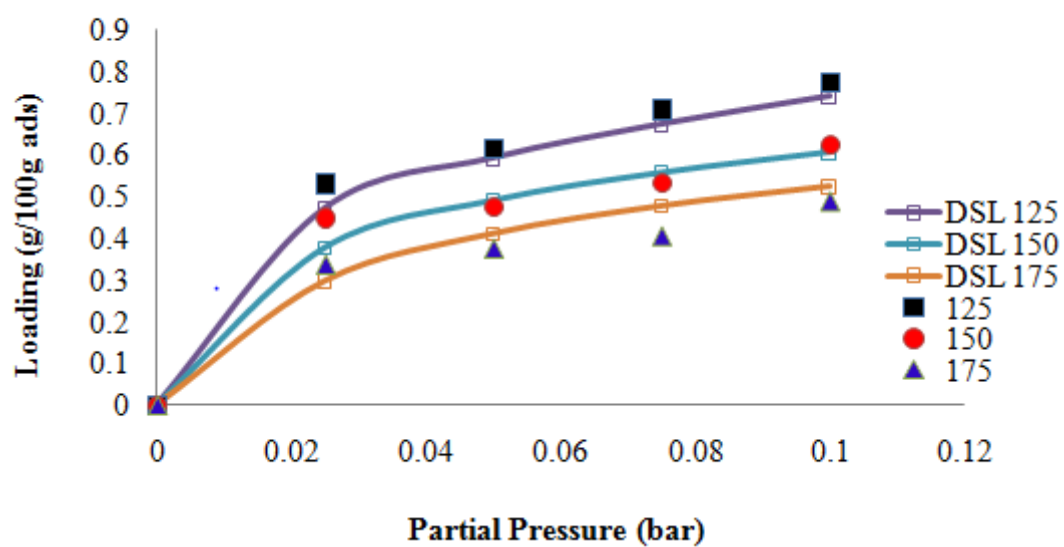


Figure 28 : Comparison of the fit of the DSL model to experimental data of the adsorption equilibrium of para-xylene.

Meta-xylene

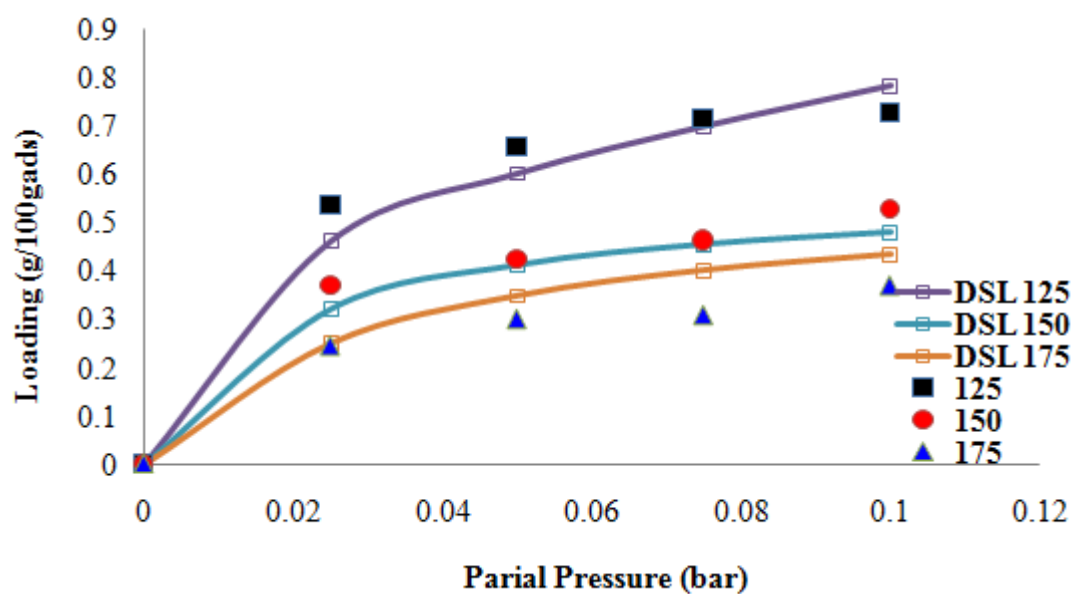


Figure 29 : Comparison of the fit of the DSL model to experimental data of the adsorption equilibrium of Meta-xylene.

Ortho-xylene

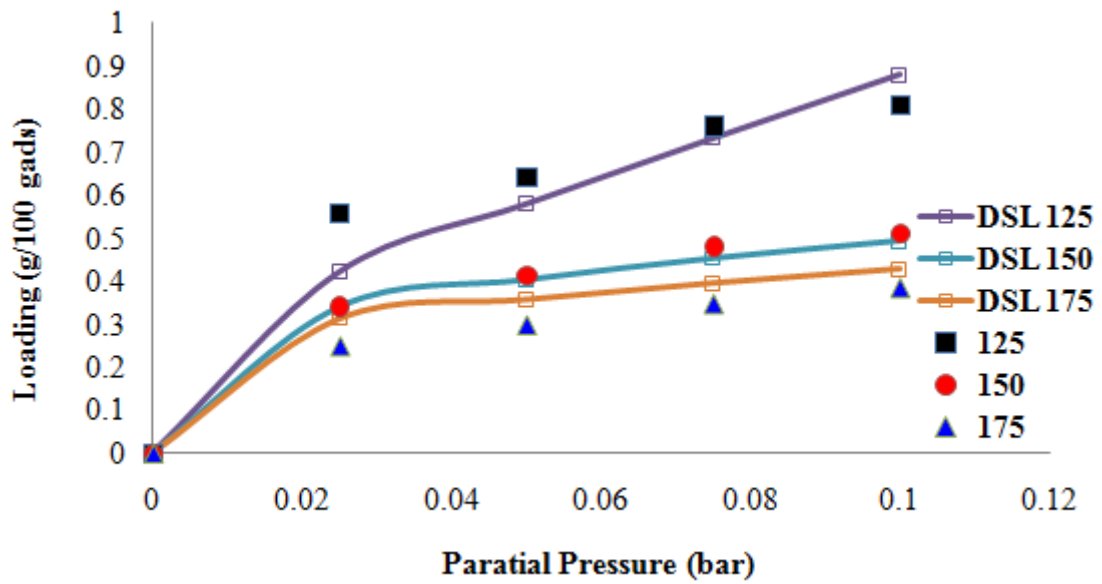


Figure 30 : Comparison of the fit of the DSL model to experimental data of the adsorption equilibrium of Ortho-xylene.

Ethylbenzene

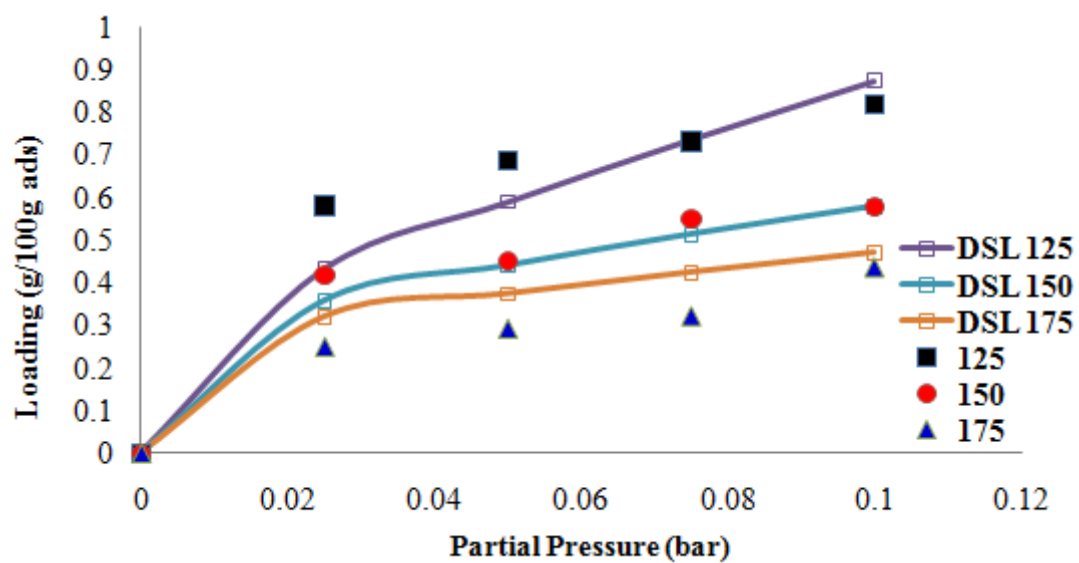


Figure 31 : Comparison of the fit of the DSL model to experimental data of the adsorption equilibrium of Ethylbenzene.

V. 6 Adsorption Enthalpies and Henry's Constant

In order to obtain the Henry constant (H) we used, the equation below, this constant can provide useful information about adsorptive processes:

$$q = Hp \quad (9)$$

Where

$$H = \frac{q}{p} \quad (10)$$

And:

H: Henry's Constant.

q: The Amount Adsorbed (g/100g_{ads}).

p: Partial Pressure.

Table 9 : Adsorption enthalpies and Henry's constants for the isomers of xylene and ethylbenzene on Zeolite beta from the DSL model.

Temperature (°C)	H (g/g _{ads} bar)			
	P-xylene	M-xylene	O-xylene	Ethylbenzene
125	7.40	8.04	8.79	7.77
150	4.95	6.08	6.35	5.36
175	4.27	4.66	5.24	4.39
ΔH_0 (kJ/mol)	24.24	42.62	50.98	35.83

Since the DSL model is the one that seems to best describe the data, the Henry constants obtained by this model were considered to be most consistent. The Henry constants are obtained in **Table 9** which clearly shows that the affinity for the adsorbent, in terms of Henry's constants, decreases in the following order: ox > mx > eb > px. From this it can be concluded that the isomer with the highest affinity to the solid is ox, and the one with the lowest affinity is px.

And it is the same conclusion for the enthalpies are decreases in the following order: ox > mx > eb > px.

Table 10 shows the selectivities between the isomers results which are calculated using the para-xylene as a reference by the following equation:

$$\alpha_{1.2} = \frac{H_i}{H_{px}} \quad (11)$$

Table 10 : Selectivities between the isomers of xylene and ethylbenzene, based on Henry's constants at 125, 150 and 175 °C, obtained by the DSL model.

Temperature (°C)	$H_i/H_{P\text{-xylene}}$			
	P-xylene	M-xylene	O-xylene	Ethylbenzene
125	1.00	1.07	1.19	1.05
150	1.00	1.23	1.28	1.08
175	1.00	1.09	1.23	1.03

VI. CONCLUSIONS

A study of xylene isomers and ethylbenzene adsorption equilibrium on zeolite BETA was shown in this work.

Two isothermal models, Langmuir and Dual-Site Langmuir, were used to interpret the adsorption equilibrium data. The DSL model gives the best fit. The parameters obtained from the model fit lead us to conclude that the quantity adsorbed increases at the lower temperature (125 °C) and decrease with the highest one (175 °C) . The selectivity is seen to be very low but we could say that there is an improvement with decreasing temperature and loading.

The validations of DSL model lead to the finding that two groups of adsorption sites may exist in this BETA zeolite for adsorbing xylene isomers.

Temperature and pressure were found to play an important role in molecular adsorption and selectivity. The temperature increase results in a decrease in adsorbed quantities.

With regards to adsorption enthalpies it is observed that the values for PX, MX, MX, and EB are similar.

In future it will be interesting to study multicomponent adsorption equilibrium data for this system in Zeolite BETA.

REFERENCES

A. Dyer. Zeolites. 2001. Editor(s): K.H. Jürgen Buschow, Robert W. Cahn, Merton C. Flemings, Bernhard Ilshner, Edward J. Kramer, Subhash Mahajan, Patrick Veyssièrè. Encyclopedia of Materials: Science and Technology. Elsevier. 9859-9863.

Ali Abughusa , Laxman Amaratunga , Louis Merceir. The recovery of rhodium ions at ultra-low concentrations using nanostructured adsorbents. 2005. Studies in Surface Science and Catalysis. 156: 957-962.

Alirio Rodrigues E., Minceva Mirjana; Modelling and simulation in chemical engineering: Tools for process innovation. 2005. Computers & Chemical Engineering. 29 (6): 1167-1183.

Anna Zaykovskaya . Synthesis and characterization of Beta zeolites for catalytic applications: influence of synthesis parameters; master theses ,2018.

Anuwattana .R ,Khummongkol . P. Conventional hydrothermal synthesis of Na-A zeolite from cupola slag and aluminum sludge.2009. Journal of Hazardous Materials. 166(1):227-32.

Baerlocher Ch., Lynne B. McCusker, D.H. Olson. Atlas of Zeolite Framework Types 6th Edition.2007. Physical Sciences and Engineering. Elsevier Science. 73- 404.

Barros M. A. S. D., Arroyo P. A and. Silva E. A . General Aspects of Aqueous Sorption Process in Fixed Beds.2013. Mass Transfer - Advances in Sustainable Energy and Environment Oriented Numerical Modeling. 10:5772-51954.

Bergeot Ghislain, Damien Leinekugel-le-Cocq, Laurence Muhr. Intensification of Paraxylene Production using a Simulated Moving Bed Reactor .2010. Oil & Gas Science and Technology. 65(5).

Brito A., Borges M.E., Otero N. Zeolite Y as a heterogeneous catalyst in biodiesel fuel production from used vegetable oil. 2007. Energy Fuels. 21: 3280–3283.

Bárcia Patrick S. and Ribeiro Ricardo M. A. Separation of Ramified Hexane Isomers with Beta Zeolite for the Enrichment of the Octane Index of Gasoline.2003. Conference. Instituto Politecnico de Bragança.

Bárcia Patrick S., Silva José A.C., Rodrigues Alirio E. Separation by Fixed-Bed Adsorption of Hexane Isomers in Zeolite BETA Pellets .2006. *Industrial & Engineering Chemistry Research*. 4 (12): 4316–4328.

Byambajav E. and Y. Ohtsuka . Cracking behavior of asphaltene in the presence of iron catalysts supported on mesoporous molecular sieve with different pore diameters. 2003. *Fuel*. 82 (13) :1571-1577.

C. Malara, G. Pierini, A. Viola. Correlation Analysis and Prediction of Adsorption Equilibria. 1992. Paperback. 10: 11-973049-9.

Cambor M.A., J. Pérez-Pariente. Crystallization of zeolite Beta – effect of Na and K-ions. 1991. *Zeolites*. 11:202 – 210.

Canadian Environmental Protection Act. Health-Based Tolerable Daily Intakes/Concentrations and Tumourigenic Doses/Concentrations for Priority Substances. 1996. Health Canada.

Christopher J. Rhodes. Properties and applications of zeolites. 2010. *Science Progress*. 93 (3) : 223-284.

Coombs Douglas, Alberto Alberti , Armbruster Thomas, Artioli Gilberto, Colella Carmine, Galli Ermanno , Grice Joel , Liebau Friedrich , Mandarino Joseph , Minato Hideo, Nickel E.H , Passaglia Eliane , Peacor Donald , Quartieri, Simona , Rinaldi Romano Ross Malcolm, Sheppard Richard , Tillmanns Ekkehart , Vezzalini, Giovanna. Recommended Nomenclature for Zeolite Minerals: Report of the Subcommittee on Zeolite of the International Mineralogical Association. 1998. *Journal Mineralogical Magazine*. 62 : 533-571.

Corma Avelino. State of the art and future challenges of zeolites as catalysts. 2003. *Journal of Catalysis*. 216 (1)–(2) : 298-312.

Davis Mark E. and Raul F. Lobo. Zeolite and molecular sieve synthesis. 1992. *Chemistry of Materials*. 4 (4): 756–768.

D.B. Broughton, C.G. Gerhold . Continuous sorption process employing fixed bed of sorbent and moving inlets and outlets. 1961. Technical Report. 298-5589.

Degnan Thomas F. Jr. Applications of zeolites in petroleum refining. 2000. *Topics in Catalysis*. 13:349–356.

Ding Lianhui , Ying Zheng. Effect of template concentration and gel dilution on crystallization and particle size of zeolite beta in the absence of alkali cations . 2007. *Microporous and Mesoporous Materials*. 103 (1)–(3): 94-101.

Daniela Sofia Domingues Guimarães. Separation of Xylene Isomers in Materials at Lavoisier Institute- Mil. 2009. Master thesis. Instituto Politecnico de Bragança.

Deckman H. W. , C. B. Roxlo, and E. Yablonovitch. 1983. Maximum statistical increase of optical absorption in textured semiconductor films. *Optics Letters*. 8 (9): 491-493

Douglas M. Ruthven. Principles of Adsorption and Adsorption Processes. 1984. *Industrial Chemistry*. 978-471.

Douglas M. Ruthven. Diffusion in zeolites. 1995. *Studies in Surface Science and Catalysis*. 97: 223-234.

Dong-Kyu Moon, Yongha Park, Yo-Han Kim, Hyungwoong Ahn , Chang-Ha Lee. Adsorption isotherms of CO₂, CO, N₂, CH₄, Ar and H₂ on activated carbon and zeolite LiX up to 1.0 MPa. 2014. *Adsorption*. 20: 631–647.

Edith M. Flanigen. Chapter 2 Zeolites and molecular sieves: An historical perspective. 2001. *Studies in Surface Science and Catalysis*. 137: 11-35.

Fabri, U. Graeser, T. Simo. Benchmark selectivity p-xylene separation by a non-porous molecular solid through liquid or vapor extraction. 2002. 10(38): 8850–8854.

Flanigen, E. M. Molecular sieve zeolite technology. 1980. *Pure and Applied Chemistry*. 52(9): 2191-2211.

Garcia Gustavo, Edgar Cardenas, Saúl Cabrera, Jonas Hedlund ,Johanne Mouzon. Synthesis of zeolite Y from diatomite as silica source. 2016. *Microporous and Mesoporous Materials*. 219: 29-37.

Garshasbi V., Jahangiri M., Anbia, M. Equilibrium CO₂ adsorption on zeolite 13X prepared from natural clays. 2017. *Applied Surface Science*. 393-225.

G. Gianetto, A Rendon, G. Fuentes . Zeolites: Features y Aplicaciones Industriales Properties. 1990. *Technological Innovation*.

Guang Guo, Hongxin Zhao. Multilevel Modeling for Binary Data. 2000. Annual Review of Sociology. 26 :441-462.

Grün M., Kurganov .A , Schacht .S, Schüth .F, Unger K.K. Comparison of an ordered mesoporous aluminosilicate, silica, alumina, titania and zirconia in normal-phase high-performance liquid chromatography.1996. Journal of Chromatography. 740 (1): 1-9.

Guisnet, M. Introduction to Zeolite Science and Technology, In Zeolites for Cleaner Technologies. 2002. Imperial College Press: London . 1-28.

Guisnet M., Ribeiro F.R. Zeólitos: um Nanomundo ao Serviço da Catálise. 2004. Fundação Calouste Gulbenkian: Lisboa .

International zeolite association. 2015. 6th International Symposium of Advanced Micro- and Mesoporous Materials. Burgas, Bulgaria.

International Zeolite Association (IZA) 20 novembro 2015.

Jeanneret J.J., A.R. Meyers. Disproportionation and transalkylation of alkylbenzenes over zeolite catalysts. 1999. Applied Catalysis A: General. 181 (2):355-398.

Joeri F. M. Denayer , Gino V. Baron. Adsorption of normal and branched paraffins in faujasite zeolites NaY, HY, Pt/NaY and USY. 1997. Adsorption. 3: 251–265.

Jungkyu Choi, Shubhajit Ghosh, Lisa King , Michael Tsapatsis. MFI zeolite membranes from a- and randomly oriented monolayers. 2006. Adsorption. 12: 339–360.

Kulasekaran Ramesh, Dendi Damodar Reddy. Advances in Agronomy. 2011. Edited by Donald L. Sparks. 113: 1-359.

Krishna Rajamani. Methodologies for evaluation of metal–organic frameworks in separation applications .2015. RSC advances.64.

Langmuir Irving. The adsorption of gases on plane surfaces of glass, mica and platinum. 1918. Journal of the American Chemical Society.40 (9): 1361–1403.

Maia, A. Á. B.; Neves, R. F.; Angélica, R. S.; Pöllmann, H. Synthesis, optimization and characterization of the zeolite NaA using kaolin waste from the

Amazon Region. Production of Zeolites KA, MgA and CaA. *Applied Clay Science* 2015, 108, 55.

Matiwaza Ncube, Yuehong Su. The removal of volatile organic compounds from supply air using a desiccant column – A theoretical study. 2012. *International Journal of Sustainable Built Environment*. 1(2) :259-268.

Meyers, R. *Handbook of Petroleum Refining Processes*. 2003 3rd edition. McGraw-Hill. New York.

Mirjana Minceva, Luis S. Pais, Alirio E. Rodrigues. Cyclic steady state of simulated moving bed processes for enantiomers separation. 2003 . *Chemical Engineering and Processing*. 42: 93-104.

Mirjana Minceva , Rodrigues A.E. Understanding and revamping of industrial SMB units for p-xylene separation. 2007. 53 (1): 138 – 149.

Moll W.L.H. Bestimmung der spezifischen Oberfläche durch Adsorption. 1954. *Kolloid-Zeitschrift*. 138 : 114–122.

Muhammad Farooq Saleem Khan, Jing Wu, Bo Liu, Cheng Cheng, Mona Akbar, Yidi Chai , Aisha Memon. 2018. Fluorescence and photo physical properties of xylene isomers in water: with experimental and theoretical approaches, *Royal Society Open Science*. 5: 171-719.

Newsam J. M., Treacy M. M. J., Koetsier W. T. , Gruyter C. B. Structural characterization of zeolite beta. *Proc. R. Soc. Lond*. 420: 375–405.

Nascimento A. R., Figueredo G. P., Silva E. M. F., Melo M. A. F, Melo D. M. A., Souza M. J. B. Synthesis, Optimization and Characterization of Zeolite Beta (BEA): Production of ZSM-5 and NaAlSiO₄ as Secondary Phases. 2017. *Rev. Virtual Quim*. 9 (4).

Nozaki Chika, Claus G. Lugmair, Alexis T. Bell, and T. Don Tilley. Synthesis, Characterization, and Catalytic Performance of Single-Site Iron(III) Centers on the Surface of SBA-15 Silica. 2002. *Journal of the American Chemical Society*. 124 (44): 13194–13203.

P.A.Wright. *Acid Catalysts*. 2001. *Encyclopedia of Materials: Science and Technology (Second Edition)* . 1-6., 2001

Shields, J.E.; Lowell, S.; Thomas, M.A.; Thommes, M. Characterization of Porous Solids and Powders: Surface Area, Pore Size and Density. 2004. Kluwer Academic Publisher: Boston, MA, USA.43–45.

Rui Li, Abolghasem Shahbazi.A .A Review of Hydrothermal Carbonization of Carbohydrates for Carbon Spheres Preparation.2015. Biological Engineering Program, Department of Natural Resources and Environmental Design.1 (1).

Sushmita Banerjee , M.C. Chattopadhyaya. Adsorption characteristics for the removal of a toxic dye, tartrazine from aqueous solutions by a low cost agricultural by-product. 2017. Arabian Journal of Chemistry. 10 (2) : 1629-S163.8.

Tanabe Kozo, Wolfgang F.Hölderich. Industrial application of solid acid–base catalysts. 1999. Applied Catalysis A: General. 181 (2) : 399-434.

Tingting Lu,Wenfu Yan, Ruren Xu , Chiral zeolite beta: structure,synthesis, and application. 2019.inorganic Chemical Frontiers. 8 (6) : 1938-1951.

Vermeiren, W.; Gilson, J.P. Impact of Zeolites on the Petroleum and Petrochemical Industry. 2009. Topics in Catalysis. 52 : 1131–1161.

Walcarius Alain, Jérôme Devoy, and Jacques Bessiere. Electrochemical Recognition of Selective Mercury Adsorption on Minerals. 1999. Environmental Science & Technology. 33 (23) : 4278–4284.

Wang, Jyue-Sheng. Oxidation of ortho-xylene to phthalic anhydride using a fluidized bed catalysis . 1965. Masters Theses.

Wenming Hao , Weimin Zhang, Zaibin Guo, Jinghong Ma and Ruifeng Li.Mesoporous Beta Zeolite Catalysts for Benzylation of Naphthalene: Effect of Pore Structure and Acidity. 2018. Catalysts. 8: 504.

Wise W.S. MINERALS Zeolites. 2005. Editor(s): Richard C. Selley L. Robin M. Cocks Ian R. Plimer. Encyclopedia of Geology. Elsevier. 591-600.

Wise W.S. Chapter MINERALS | Zeolites. 2013. In book: Reference Module in Earth Systems and Environmental Sciences..

Xomeritakis, G., Lai, Z., Tsapatsis, M. Separation of xylene isomers vapors with oriented mfi membranes made by seeded growth. 2001. *Ind. Eng. Chem. Res.* 40 : 544–552.

Yaqiong Qiu , Xin Lu, Tao Pang, Shukui Zhu, Hongwei Kong, Guowang Xu. Study of traditional Chinese medicine volatile oils from different geographical origins by comprehensive two-dimensional gas chromatography-time-of-flight mass spectrometry (GCxGC-TOFMS) in combination with multivariate analysis. 2007. *J Pharm Biomed Anal.* 43(5):1721-7.

Yan Y., Davis M., Gavalas G. Preparation of zeolite ZSM-5 membranes by in-situ crystallization on porous α -al₂o₃. 1995. *Ind. Eng. Chem. Res.* 34 : 1652–1661.

Yuan W., Lin Y., Yang W. Molecular sieving mfi-type zeolite membranes for pervaporation separation of xylene isomers. 2004. *J. Am. Chem. Soc.* 126 : 4776–4777.

Yuxi Yang, Peng Bai, and Xianghai Guo..Separation of Xylene Isomers: A Review of Recent Advances in Materials. 2017. *Industrial & Engineering Chemistry Research.*, 56(50): 14725–14753.

Zeid A. ALothman. A Review: Fundamental Aspects of Silicate Mesoporous Materials.2012. *Materials.* 5: 2874-2902.